Reprogramming human peripheral blood mononuclear cells to inducible pluripotent stem cells (hiPSC): An examination of the efficacy of different methods

by

Elham Afshinmanesh

B.Sc., University of Tehran, 2008

Thesis Submitted in Partial Fulfillment of the
Requirements for the Degree of
Master of Science

In the

Department of Biomedical Physiology and Kinesiology

Faculty of Science

Elham Afshinmanesh 2016

SIMON FRASER UNIVERSITY

Summer 2016

Approval

Name:	**Elham Afshinmanesh**
Degree:	**Master of Science**
Title:	***Reprogramming peripheral blood mononuclear cells to inducible Pluripotent Stem Cells (hiPSC): An examination of the efficacy of different methods***
Examining Committee:	**Chair:** Dr. Damon Poburko Assistant Professor

Dr. Glen F. Tibbits
Senior Supervisor
Professor

Dr. Jonathan Choy
Supervisor
Associate Professor
Department of Molecular Biology and Biochemistry

Dr. Tomath Claydon
External Examiner
Associate Professor

Date Defended/Approved: 28 July 2016

Ethics Statement

The author, whose name appears on the title page of this work, has obtained, for the research described in this work, either:

a. human research ethics approval from the Simon Fraser University Office of Research Ethics

or

b. advance approval of the animal care protocol from the University Animal Care Committee of Simon Fraser University

or has conducted the research

c. as a co-investigator, collaborator, or research assistant in a research project approved in advance.

A copy of the approval letter has been filed with the Theses Office of the University Library at the time of submission of this thesis or project.

The original application for approval and letter of approval are filed with the relevant offices. Inquiries may be directed to those authorities.

Simon Fraser University Library
Burnaby, British Columbia, Canada

Update Spring 2016

Abstract

Modeling a disease “in a dish,” a new research tool to study human heart disease mechanisms, is becoming as popular as more established techniques such as the use of transgenic mice. The primary practical challenge of this “disease in a dish” method is efficiently directing human induced pluripotent stem cell (hiPSC) differentiation into the desired lineages, with the major concern being the variability within hiPSC clones.

To generate a reliable *in vitro* model for inherited cardiac diseases and address the variability problem, characteristics of hiPSCs derived from the blood of four human donors using both the episomal and Sendai virus reprogramming systems were examined. The hiPSC-cardiomyocytes (hiPSC-CMs) generated were then characterized according to their cardiac-specific gene expression properties. No differences were observed on the effect of the reprogramming system on expression of pluripotent genes in iPSCs but differences were observed in expression of cardiac specific genes in cardiomyocytes derived from those iPSCs despite a high variance in the analysis.

Dedication

To my parents Safieh and Mohsen for their indefinite love and support.

Acknowledgements

My deep gratitude goes first to my senior supervisor Dr. Glen Tibbits for accepting me to participate in the iPSC project and his enormous support along the way. To my supervisory committee member Dr. Jonathan Choy for his critical comments on my project and his generosity in sharing his laboratory facilities with me to carry out my project.

To Sanam Shafaattalab for teaching me the cell culture techniques required for running this project. Dr. Anna Von Rossum for teaching me T-cell culture and flow cytometry. To Timothy Heslip for his help in flow cytometry set-up. To Dr. Cynthia Gershome for providing me insight in troubleshooting. To Dr. Damon Poburko for teaching me imaging and image analysis. To my friendly and helpful laboratory members Marvin Gunawan, Kaveh Rayani, Valentine Sergeev, Dr. Charles Steven, Dr. Christine Genge and Colin Peters.

My special thanks goes to Deidre de Jong-Wong for being the most helpful and supportive editor while I was writing my thesis.

I was fortunate to work with all of these wonderful people and I would like to thank everyone in the Molecular Cardiac Physiology Group (MCPG) in the department of Biomedical Physiology and Kinesiology at Simon Fraser University.

Table of Contents

List of Tables

List of Figures

List of Acronyms and Abbreviations

Term	Initial components of the term
bFGF	Basic fibroblast growth factor
eGFP	Enhanced green fluorescent protein
ESC	Embryonic stem cell
hiPSCs	Human induced pluripotent stem cells
MEF	Mouse embryonic fibroblast
MOI	Multiplicity of infection
PBMCs	Peripheral blood mononuclear cells
SeV	Sendai virus
TCR	T-cell receptor

Glossary

Term	Definitions
Feeder layer	Cells used in co-culture to maintain pluripotent stem cells by releasing nutrients into the culture media and providing a sticky surface to which the stem cells can attach.
MOI	The ratio of viruses to infected cells in a specified area.
Nucleofection	A rapid and efficient non-viral transfection method that enables the in vitro transfer of nucleic acids into cells by applying a specific voltage in the presence of specific reagents.

Chapter 1. Introduction

1.1. Stem cell hierarchy

The term “stem cell” first appeared in scientific literature in 1868, when biologist Ernst Haeckel used the words to describe the single celled organism that was the ancestor cell to all life on Earth. Since that first reference, the definition of stem cell has been refined to refer to cells that possess two remarkable features; the capacity for self-renewal and the potential for differentiation into disparate specialized cell types[1].

Stem cells can be derived from both embryonic and postnatal animal tissues and exhibit a broad range of developmental potency. This attribute ranges from totipotent, which has the potential to give rise to all embryonic and extra-embryonic cells and tissues to unipotent which are limited to differentiating into only one cell type[2]. The totipotent[3] stage of stem cells begins with the zygote (shortly after the fusion of oocyte and sperm) or its artificial counterpart, the clonote[4] (created by removing the somatic nucleus and inserting it into an enucleated oocyte) and extends to the blastomer (the first division of the zygote or clonote).

The blastomer[5] loses its totipotency once it divides into the 32-cell structure called the morula. Cells forming the morula and the structures that develop from it, the blastocyst and the inner cell mass (ICM), are pluripotent and are able to differentiate into any of the three germ layers; the mesoderm, the ectoderm and the endoderm[6]. The primary difference between a totipotent and pluripotent stem cell is the totipotent cells’ ability to also differentiate into placental tissue, something the pluripotent cells cannot do[2,7].

Germ layer cells are multipotent and can give rise to multiple but limited, specialized cell types such as those present in a specific tissue or organ. Most adult stem cells are multipotent, able to generate the mature cell types of their tissue of origin[8].

On the stem cell potency continuum, the final, most limited cells are the unipotent stem cells, which can only differentiate into a single cell lineage[2].

In the fields of regenerative medicine and drug discovery, pluripotent stem cells, which can differentiate to three germ layers both *in vitro* and *in vivo*[9], are viewed as the ideal candidate cells for therapeutic and research purposes. However, the use of pluripotent human embryonic stem cells (hESCs) extracted from developing embryos is not only ethically controversial but the *in vivo* immunogenicity features of these cells often limit their clinical applications[10]. The recent technological development of human induced pluripotent stem cells (hiPSCs), which are generated from already differentiated cells[11-13], do not present the hESC obstacles and are amenable for use in the personalized medicine approach to developing unique therapies for inherited diseases.

1.2. IPSCs as a platform for human disease models

To date, because mammalian genomes have a high level of evolutionary conservation[14], animal models such as mice, rats and non-human primates have been used as tools to model human disorders. The animal models facilitate the study of disease mechanisms at different developmental stages in a variety of cell types. Although the mouse model in the past decade or so has become the most frequently used animal model to mimic human diseases due, in large part, to transgenic technologies, it has some significant structural and functional differences compared to humans. The differing organ functions of mice and humans inhibits the modeling of some human disease phenotypes in the mouse[15]. In the worst-case scenario, the same genotype can be lethal in one species and viable in the other; for example, mice with monosomy X can survive but this aneuploidy is embryonically lethal in humans[16].

To this end, hiPSCs are viewed as an important new tool for the modeling and study of human diseases. The primary advantages hiPSCs have over the mouse and other mammals is that the cells are: 1) human (and carry the genotype of the donor) and 2) readily amenable to genome editing (e.g. CRISPR). As well, hiPSCs are cell-lines which have indefinite self-renewal capabilities and can differentiate into any human cell type[17],

allowing not only genotype-phenotype relationship studies of human disorders but also the generation of the large numbers of cells necessary for drug screening and cell therapy.

The types of diseases that can be modeled using hiPSCs must meet certain criteria. The hiPSC model is ideal for the study of monogenic diseases (diseases arising from a single gene modification), such as Lesch-Nyhan disease[18]. The disease should also show high penetrance within the human population, have an early onset during development and be associated with a clear cellular phenotype[17]. Meeting these criteria will likely result in an observable *in vitro* phenotype using the hiPSC model.

Cell types generated from pluripotent stem cells more closely resemble the fetal state of those cell types rather than the adult one[19-21], meaning hiPSCs are more suitable for modeling disorders that appear during fetal development or early childhood[17]. Two examples of these disorders are Down and Turner Syndromes which affect embryogenesis and cause high miscarriage levels[22,23].

1.2.1. Cardiovascular disease models and hiPSC-derived cardiomyocytes

HiPSCs are of particular interest to researchers in the field of cardiovascular personalized or precision medicine in which the aim is to uniquely prevent or treat cardiac diseases based on individual variability[24]. This field of medicine endeavours to answer fundamental questions such as why do patients with the same genetic mutation respond differently to the same clinical treatment and “why are some patients with a particular genetic mutation at higher risk of complications than others? Studying the process of diseases at the molecular or cellular level may provide answers.

However, invasive surgical procedures have been required to obtain adult cardiomyocytes (CMs) and establish primary cells in culture[25] and prolonged *in vitro* maintenance of these cells is not currently feasible. For these reasons, hiPSCs are an exciting new tool to generate unlimited amounts of patient-specific CMs which can mimic their endogenous counterparts and act as integrators[25]. For example, by exposing hiPSC-derived CMs to environmental perturbations *in vitro*, cardiac researchers can integrate the

patient's genomic disease susceptibility with specific environmental influences to simulate the patient's condition[25].

HiPSCs are used primarily to model cardiovascular diseases such as arrhythmia syndromes and channelopathies which have clear, and easily assessable phenotypes, both *in vitro* and *in vivo*[25]. Two of the most commonly modelled cardiac diseases are Familial Long QT Syndrome (LQTS) which is caused by prolonged ventricular action potential duration in patients[26] and Catecholaminergic Polymorphic Ventricular Tachycardia (CPVT) which can lead to a life-threatening arrhythmia under emotional stress and/or physical exertion[26].

HiPSC-CMs can be used to model cardiac diseases and enable assessment of proarrhythmic risks. By expressing important ion channels, hiPSCs-CMs retain the complexity of the human action potential generation, allowing detection, assessment, and prediction of proarrhythmic risk. In addition, hiPSC-CMs can be derived from patients with various types of heart disease, enabling the investigation of the susceptibilities of specific cardiac diseases to drug-induced arrhythmia. There are several risk factors (genetic predisposition, being female, and the presence of structural heart disease)[27] that can influence drug-induced arrhythmias and hiPSC-CMs provide a unique platform to investigate these risk factors at the cellular level. Finally, hiPSC technology can enhance the development of drugs based on patient-specific differences at the cellular level[25].

1.3. Generating hiPSCs and the role of transcription factors

To generate hiPSCs reprogramming factors are essential. Reprogramming or transcription factors are genes that are normally expressed in the early stages of embryonic development and are involved in the maintenance of the pluripotency and self-renewal of stem cells. Before the early 2000s, it was known that already differentiated somatic cells could be reverted back to pluripotency if its nucleus was implanted into an enucleated egg[28-30]. However, it was unclear if an intact differentiated somatic cell could be reprogrammed back to a pluripotent state. To answer this question, in 2006, Yamanaka and his colleagues focused on transcriptional factors known to aid in the maintenance of pluripotency in embryonic stem cells. He and his team screened

a pool of 24 pluripotency-associated factors, introducing the genes into skin fibroblasts and studying the resulting colonies. Some of the colonies generated had embryonic stem cell characteristics. Next, Yamanaka attempted to determine the minimal number and which combination of transcriptional factors was required to reprogram adult cells into pluripotent cells[31,32]. They determined, first in mice and subsequently in humans, that four transcription factors: Octamer-binding protein 4 (Oct4; also known as POU5F1); Sox2; Myc proto-oncogene protein (c-MYC); and Kruppel-like factor 4 (Klf4) [32] were required. In target somatic cells, such as the fibroblasts that Yamanaka et al. used or the peripheral mononuclear blood cells (PBMCs)[13,33,34] used by Fukuda's group, the overexpression of these four genes causes the silencing of expressed somatic genes and the up-regulation of genes normally expressed only in embryonic stem cells.

These four pluripotency factors function as lineage-specific master transcription factors that reset the epigenetic and transcriptional state of the differentiated cells to that of pluripotent cells. The resulting iPS cells exhibit embryonic stem cell features, including the expression of pluripotent genes such as Nanog[35], the ability to develop into different embryonic tissues, and the formation of teratomas upon injection into immunocompromised mice[32].

Through the overexpression of the four Yamanaka transcription factors, iPSCs have since been derived not only from different types of human cells but also from different species including human[36], rat[37], mice, and rhesus monkey[38]. This indicates that the transcriptional network leading to reprogramming is strongly conserved across species[39-43].

1.4. HiPSCs and reprogramming systems

Generating robust human iPSCs and following that, successfully differentiating them into a specific cell type, is a nascent technology that is just a little over a decade old. As such, developing efficient and reproducible reprogramming strategies is a burgeoning field. Although the importance of the four Yamanaka transcription factors--Oct4, Sox2, Klf4, and c-Myc--have been identified, other elements such as determining appropriate adult human

somatic cell sources, vectors and reprogramming cocktails are still in the process of being optimized and standardized.

1.4.1. Human somatic cells as a source of iPSCs

Choosing which cell type to begin with prior to initiating reprogramming experiments is critical. Important criteria to consider include the availability of the cell type, its demonstrated or predicted ease of reprogramming and its yield efficiency. Although cells from embryonic or juvenile tissues may considered ideal candidates due to their low accumulation of genetic mutations compared to adult somatic cells, obtaining them is accompanied with the possible distortion or destruction of the embryo[44]. This is ethically controversial and has led to the consideration of other cell types, specifically those from adult tissues[45].

Currently, the two of the most widely used, terminally differentiated, human adult somatic cells used for reprogramming to iPSCs are dermal fibroblasts and peripheral blood mononuclear cells (PBMCs). In addition, hiPSCs have been generated from other sources such as human urine[46]. However, both dermal fibroblasts and urine cells have limitations. Urine cells show a marked reprogramming efficiency decrease after five passages[47] and deriving dermal fibroblasts from donors requires relatively invasive procedures and several weeks to establish a primary cell cultures from the skin biopsy[36,48]. In contrast, taking a small volume of blood from donors is non-invasive and sufficient for the isolation of PBMCs which takes less than an hour to complete[13,33]. These characteristics make PBMCs a preferred human cell source.

1.4.2. Integrative reprogramming methods

Integrative reprogramming methods were developed based on activating the endogenous, silent pluripotent genes in somatic cells. Infecting mouse or human fibroblasts with the four Yamanaka transcription factors—Oct4, Sox2, Klf4, and c-Myc- was first achieved in 2006-2007[32,36], using Moloney murine leukaemia virus derived retroviruses. In retroviral protocols, transgenes remain in the generated hiPSCs, where they can randomly integrate into the genome of the host cells, modifying the host genes and affecting transcription[36]. Additionally, there is the possibility that the transgenes'

transcription can resume in the differentiated cells derived from hiPSCs [49]. As a result, in clinical trials, the use of hiPSCs derived from this method is not recommended, particularly if the derived cells are to be introduced into patients. The generation of transgene-free hiPSCs is not only essential for potential therapies and clinical applications, but also for the development of reliable *in vitro* models that accurately emulate human diseases[50,51].

1.4.3. Non-integrative reprogramming methods

To overcome the major limitation of integrative iPSC generation—the potential for permanent genetic modification resulting from the integration of retroviral vectors into the genomes of somatic cells--non-integrative reprogramming methods were developed. There are currently four main non-integrative reprogramming methods: integration-defective viral delivery; episomal delivery; RNA delivery; and protein delivery[52-56]. The two most efficient non-integrative methods of reprogramming PBMCs are the temperature-sensitive mutated Sendai virus system[50] (an integration-defective viral delivery method) and the episomal system as shown in Figure 1.1.

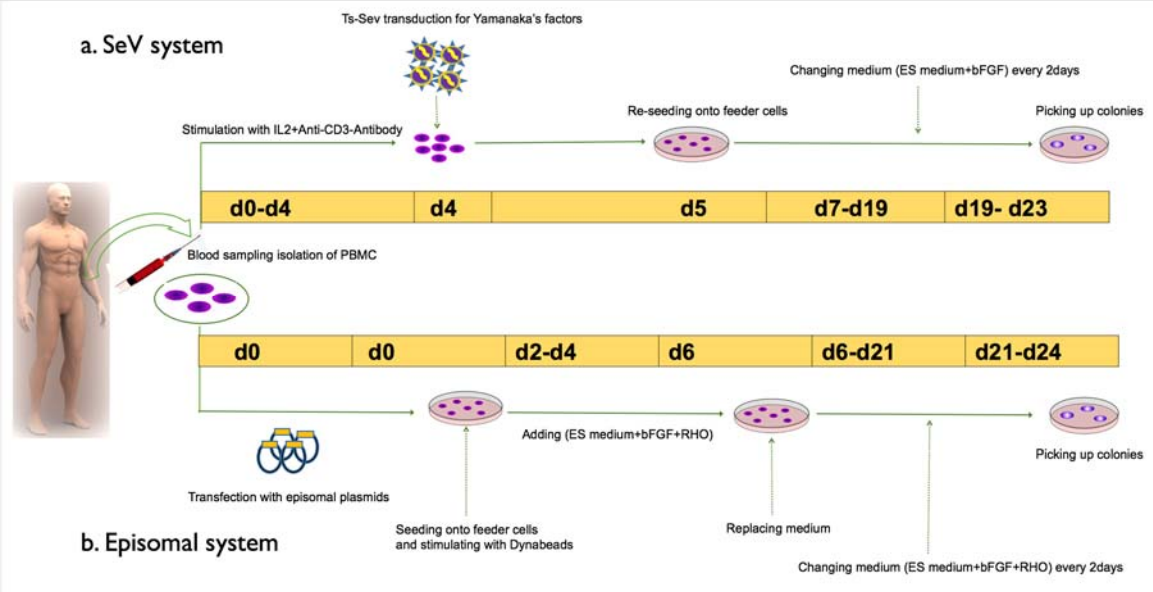

Figure 1.1 Reprogramming systems:
a) Sendai-virus (SeV) reprogramming system
b) Episomal-plasmid reprogramming system

1.4.3.1 Sendai virus system

The first effective non-integrative method for reprogramming PBMCs utilizes the Sendai virus (SeV) [50,57]. This virus is derived from the *Paramyxovirdae* family and is an enveloped virus with a 15 kb single-stranded, negative-sense, non-segmented RNA genome[58]. Most importantly, replication of a recombinant SeV vector is independent of the host cell's genome and occurs in the cytoplasm of the infected cell[59]. SeV vectors have been shown to be able to efficiently introduce foreign genes into a wide spectrum of host cell species and tissues [60].

However, while SeV vectors are able to efficiently generate iPSCs from human fibroblasts [50] and human blood cells,[34] they cannot be removed from the host cells unless an anti-SeV-HN antibody is introduced. "Footprint free" temperature-sensitive (TS) SeV vectors have since been designed and are now considered to be superior alternatives for generating vector-free iPSCs[54]. TS-SeVs have mutations in their RNA polymerase structures, causing silencing or degradation of the viruses above their permissive temperatures (for example, above 37^{o}C), leaving the iPSCs transgene free[54]. The most efficient TS-SeV vector system available to date, CytoTune-iPS 2.0 (ThermoFisher), contains the Oct4, Sox2, and Klf4 genes in a single polycistronic vector, c-Myc in a separate vector and an additional Klf4 vector which serves to enhance the system's efficiency. Ts-SeV vectors provide a robust, non-integrative system with high efficiency and fast viral clearance from generated iPSCs.

1.4.3.2 Episomal system

A second relatively effective, non-integrative method for reprogramming PBMCs uses episomal vectors. These plasmids have been constructed as either an all-in-one single plasmid containing all the four Yamanaka transcription factors[56] or as separate plasmids, each containing one of the fours transcription factors[53]. With the help of a generated electrical field (electroporation), these plasmids can directly enter the host cell's nucleus.

One drawback of the episomal system is that it is not as efficient as the viral reprogramming methods, possibly due to the large size of the episomal plasmids (5-10 kb), which may mean that fewer host cells are able to receive the appropriate dose of

plasmids during reprogramming. The early dilution of the plasmids in actively proliferating cells and the downregulation of reprogramming factors[61] in mammalian cells because of silencing of prokaryote sequences contained in the backbone of these episomal vectors are two other factors decreasing the efficiency of episomal system.

To overcome the need for serial transfection due to dilution of episomes through cell division, oriP/Epstein-Barr nuclear antigen-1-based episomal vectors were designed [53]. Although these plasmids can transfect human cells, their transfection efficiency is extremely low (3 to 6 colonies per million nucleofected cells) due to the large size of the plasmids (more than 12 kb). As well, their maintenance and stability in transfected cells requires drug selection. Okita et al[62,63] has enhanced the transfection efficiencies of episomal plasmids by adding the p53 suppressing gene and substituting L-Myc (which is more potent) instead of c-Myc. The highest transfection efficiency in human PBMCs has been obtained by co-transfection of four plasmids (Oct4-shp53, L-Myc-LIN28, Sox2-Klf4 and an EBNA-1 vector), in which Shp53 suppresses the activity of the regulatory protein P53 while EBNA1 is an essential factor for the episomal amplification of vectors[62,63]. However, even with these enhancements, the episomal system remains less efficient than the viral reprogramming methods.

1.5. Molecular mechanism of reprogramming

Although numerous methods have been developed to improve the introduction of reprogramming factors into somatic cells, the embryonic stem cell-like cells generated are different in expression levels of pluripotency-associated genes[64,65] and only a small percentage of them develop into fully reprogrammed cells. The reasons for these discrepancies and low efficiencies are largely unknown.

To date, it also remains unclear exactly how the expression of transcription factors functions to erase the somatic cells' program and confers pluripotent capabilities through the establishment of an ESC-like transcriptional network. What little is known about the three phases of reprogramming (initiation, the intermediate phase, and maturation and stabilization) and the modifications that occur in the epigenetic and gene expression

networks of the reprogrammed somatic cells in these phases is described in the following sections.

1.5.1. Phases of reprogramming

The three phases of reprogramming-initiation, the intermediate phase, and maturation and stabilization--have primarily been studied using fibroblasts as the somatic cell model.

1.5.1.1 Initiation phase

The first wave of reprogramming is initiated by many events occurring either sequentially or in parallel. The four introduced transcription factors, also known as the ectopic OSKM (Oct4, Sox2, Klf4 and Myc), generate a hyper-dynamic chromatin state by binding to many regions of the host fibroblast's genome that are not normally OSKM targets in ESCs. This initiates stochastic gene expression[66] causing increased cell proliferation[67,68]; introduces histone modifications on somatic genes causing loss of the somatic cell's epigenetic programming[36,69,70]; initiates mesenchymal-to-epithelial transition [71-73] causing the start of morphological changes; inhibits apoptosis and senescence (aging); and alters the cell metabolism. The initiation phase occurs between day 0 and day 3 after introduction of the Yamanaka transcription factors[74].

1.5.1.2 Intermediate phase

Following the initiation phase, the cells containing the four introduced transcription factors enter the intermediate phase, transitioning through an unknown rate-limiting step that leads to a long latency period of 4 to 9 days after introduction of the transcription factors. In this step, due to the stochastic activation of pluripotency markers[66], a temporary activation of developmental regulators and glycolysis takes place. IPSC predictive markers, including undifferentiated embryonic cell transcription 1 (Utf1), estrogen-related receptor beta (Esrrb), developmental pluripotency associated 2 (Dppa2), and Lin28, activate in a small subset of cells[66].

1.5.1.3 Maturation and Stabilization phase

Cells that express the iPSC predictive markers in the intermediate phase enter the last phase of reprogramming through the activation of Sox2[68]. This directly or indirectly triggers a series of deterministic events-that include activation or silencing of different combinations of genes that must occur in a particular order to lead to the generation of iPSCs[75,76]. In this phase, the cell eventually stabilizes into the pluripotent state which includes silencing of the transgenes, remodelling of the cytoskeleton to an ESC-like state, resetting of the epigenetic state and activation of the core pluripotency network (Oct4, Sox2, Nanog)[66,74,77,78]. This late phase starts after day 9 with the end of the process occurring around day 12[74].

1.6. T-cell activation

T-cells are the primary reprogramming target of all the cell types making up PBMCs. Their easy proliferation in culture and their high efficiency induction with pluripotency genes are two important features necessary for the successful reprogramming of mature cells to iPSCs. However, in order to achieve efficient levels of T- cell reprogramming, T-cell activation is key, not only for increasing the number of T-cells but also magnifying the uptake of pluripotency genes [33,79]. *In vivo*, the events initiating the transition of naïve T-cells from a quiescent to an activated state are called cell priming [80]. *In vitro*, cell priming can be recapitulated using anti-CD3 monoclonal antibodies and interleukin-2 (IL-2) [81,82].

In the SeV reprogramming system, T-cells can be selectively activated in PBMC cultures via interaction of the T-cell receptor complex with anti-CD3 plate bound antibodies. This stimulates signalling pathways required for T-cell activation [80], enabling the now activated T-cells to express IL-2 and IL-2 receptors, which are required for cell division [81]. However, activated T-cells are prone to undergo activation-induced cell death shortly after activation [83]. To prevent this and to encourage proliferation and longer survival time, high concentrations of IL-2 (175 U/ml) can be maintained in the medium[33,84]

In the episomal reprogramming system, T-cells can be selectively activated after nucleofection of PBMCs with episomal plasmids carrying pluripotency transcription

factors. T-cells can be stimulated, immediately following nucleofection, with immunomagnetic beads coated with anti-CD3 and anti-CD28 monoclonal antibodies and maintained in low concentrations of IL-2 (30 IU/ml) [63,85]. Anti-CD28 monoclonal antibodies can be included as CD28 has been identified as a co-stimulator that may amplify T-cell receptor (TCR) signalling to induce proliferation and IL-2 production in T-cells[86].

Although much is known about the requirements for T-cell activation both *in vivo and in vitro*, protocols are still in the process of being optimized for hiPSC generation.

1.7. High level of variability in iPSCs

Because iPSC technology is so young, not only are there many questions about T-cell activation and the molecular mechanisms of reprogramming, there are other aspects of pluripotency which are not clearly understood either. For example, studies on single pluripotent cells and on populations of pluripotent cells have revealed that the pluripotent state is a statistical property of stem cell populations and is not well defined at the single cell level[87].

The functionality of pluripotent cells can be experimentally assessed using different criteria including their ability to differentiate *in vitro* into cell types of all three germ layers, their ability to form teratomas in mice *in vivo*, or their development after introduction into embryos[88]. Although these assays distinguish between functional pluripotent cell populations and non-pluripotent cell populations, they do not assess the pluripotency of individual stem cells.

Studies, which used high-throughput single-cell gene expression profiling, have discovered a remarkable degree of cell-to-cell variability in the expression of key transcription factors such as Nanog, ZFP-42 and Klf4 within functionally homogenous pluripotent stem cell populations[57,89-92]. However, despite intracellular expression fluctuations in which individual cells transit stochastically between states in dynamic equilibrium, the overall structure of the population remains stable[91]. Interestingly, although a population of cells derived from a single stem cell colony may appear to be functionally homogeneous, it will likely be different from cell populations derived from other colonies

due to their unique stochastic expression of pluripotent genes. There is a large degree of variability not only between cells of a single population but also between different populations of cells, all depending on the pluripotent genes' levels of expression. This variability has serious implications for future research and clinical applications.

1.7.1. Cardiogenesis *in vivo* and *in vitro*

Once hiPSCs have been generated, their differentiation into cardiomyocytes (CMs) is the next critical step for cardiac researchers. However, while the general roadmap of differentiation to adult cardiomyocyte from embryonic tissue has been well described in the field of developmental biology, the detailed molecular mechanisms of these signalling pathways are still unresolved. Once these mechanisms are understood, directing iPSCs derived from patients with inherited cardiac diseases towards cardiac lineage differentiation will be more reproducible. This is the goal, to be able to generate a reproducible cardiac model enabling personalized therapeutic medicine for these patients.

Cardiogenesis in an embryo begins at gastrulation, when the endoderm and mesoderm are formed. Mesoderm exposed to fibroblast growth factor and bone morphogenetic protein (BMP), coupled with inhibition of the Wnt pathway, becomes precardiac, the precursor of the heart tube [93-95]. This single layer of the heart tube is capable of wave-like contraction and encodes the contracting cardiac protein troponin. As the embryo grows, the heart matures and the conduction system develops, thus contractility increases and electromechanical coupling transforms from an autonomous wave-like propagation to a nodal-regulated mature conduction system[96-99]. Commensurate with this is the expression of the proteins making up the cardiac contractile machinery[71].

1.7.2. Human cardiac troponin complex and myosin light chain

Among cardiac-specific proteins, the troponin complex with its three subunits, troponin T, C, and I, plays a crucial role in the generation and regulation of contraction in cardiac cells. Mutations in the troponin subunits can lead to different types of cardiomyopathy; in particular, mutations in troponin T and I have been associated with

heart failure and sudden cardiac death. As a result, the troponin complex has been the target for some cardiotonics[100] (drugs that improve the contraction of the heart muscle) in the treatment of heart failure and is the current subject of extensive cardiac research.

In humans, there are three paralogs of troponin I (TnI); the fast and slow skeletal paralogs and the cardiac paralog [101-103]. The slow skeletal TnI (*TNNI 1*) is expressed in cardiac muscle during embryonic development[104-106] and, within 1-2 years after birth, is replaced by the cardiac isoform of troponin I (*TNNI3*) [107-109]. Measuring the expression of these two paralogs provides a reliable indication of whether the hiPSC-derived CMs are similar to adult or fetal CMs. Another subunit of the troponin complex, troponin T (TnT) also has three isoforms in humans; the slow and fast skeletal isoforms and the cardiac isoform[110,111]. An increased level of mRNA of the slow skeletal isoform of TnT in fetal heart muscle,[112] without any evidence of translation[113-115], has been observed. The only isoform of TnT detected in the adult human heart is the cardiac isoform. By measuring the RNA for the slow skeletal and cardiac isoforms of TnT in hiPSC-derived CMs, the developmental status, fetal or adult, of those cells can be determined.

The cardiomyocytes derived from hiPSCs can be chamber specific meaning cardiomyocytes with either an atrial or ventricular phenotype. One method to determine the presence of these two phenotypes is to measure the relative expression levels of the two paralogs of myosin light chain 2 (atrial - MLC-2a and ventricular -MLC-2v).

1.8. Description of this Master's project

In 2006, Yamanaka and his colleagues identified four transcription factors that could reprogram an adult somatic cell to become an induced pluripotent stem cell--an iPSC-- and from that turning point, the technology to reliably and productively generate hiPSCs has rapidly developed. The ability of hiPSCs to serve as *in vitro* models for human diseases, especially the monogenic diseases, is revolutionary, as is their potential use in drug development, personalized clinical therapies, and regenerative medicine. Of particular interest is the potential for hiPSCs to elucidate and eventually treat cardiac diseases such as atrial fibrillation or Long QT syndrome.

PBMCs from blood have been identified as an easily available, non-invasive source of human somatic cells that can be manipulated, through either episomal or SeV non-integrative reprogramming systems, to become hiPSCs. However, there is much to learn. Currently, there is little understanding of the molecular mechanism of reprogramming; the efficiencies of the non-integrative reprogramming systems are both low (0.01 to 0.1% at maximum) and the level of variability at the cell-to-cell level of hiPSCs is high. While PBMCs, specifically the T-cells, can be successfully reprogrammed to become hiPSCs and then differentiated into CMs (either atrial or ventricular) there remain critical questions about the efficiency of the reprogramming methods and the quality and reproducibility of the generated CMs.

This Master's research project addressed two of these questions; which reprogramming system--the episomal or the SeV--is more effective at generating hiPSCs from PBMCs and what hiPSC characteristics reliably indicate future successful differentiation to CMs.

Before the questions could be answered however, a T-cell activation protocol had to be developed and optimized, followed by optimization of both the SeV and episomal reprogramming methods. Only then could hiPSCs be generated. Next, these hiPSCs were characterized for pluripotent surface markers and intracellular pluripotency gene expression at early (passage 5) and late passage (passage 10). The functionality of the hiPSCs, that maintained their pluripotency to passage 10, were then assessed for their successful differentiation to CMs as measured by the levels of expression of cardiac-specific gene markers.

The aims that were addressed in this research project are integral to the development of an effective patient-specific hiPSC model.

Chapter 2. Materials and Methods

2.1.1. Human cell isolation and culture

Human whole blood was obtained from four healthy donors - two males and two females between 20-30 years old -whose written informed consent is in accordance with the Simon Fraser University Ethical Review Board's guidelines (see Appendix A). The blood was collected by venipuncture into BD Vacutainer tubes (BD Biosciences,) containing an anticoagulant citrate dextrose solution. Peripheral blood mononuclear cells (PBMCs) were aseptically isolated at room temperature immediately following collection using Sepmate tubes (STEMCELL Technologies) according to the manufacturer's instructions.

To begin the selective expansion of T-cells within each PBMC culture, a 24-well plate (Corning) was first coated with 250 µl /well anti-human CD3 antibodies (eBioscience) dissolved in 1 ml D-PBS (Life Technologies) for a final concentration of 10 µg/ml and incubated in 37°C for a minimum of one hour. Wells were next washed twice with 0.5 ml D-PBS after coating and the D-PBS aspirated. Then, 5 x 10^5 PBMCs in 500 µl T-cell medium [RPMI (Lonza) containing 10% FBS (Life Technologies) and 175 U/ml IL-2 (Peprotech)] were added to each well of the coated plate and the plate was incubated at 37°C.

2.1.2. Trypan blue exclusion assay

To determine the number of viable cells present in PBMC cultures before and after T-cell stimulation, the Trypan blue exclusion assay was used. In triplicate experiments, 5 x 10^5 live cells were stimulated with plate-bound anti-human CD3 antibodies (10 µg/ml, eBioscience; see Section 2.1. 1 for plate coating protocol) in 500 µl T-cell medium [RPMI (Lonza) containing 10% FBS (Life Technologies) and 175 U/ml IL-2 (Peprotech)] and incubated at 37^{o}C. The number of live cells was counted daily, over a period of one week. To count, 10 µl cells were pipetted from the PBMC culture and stained with Trypan blue (Lonza) for 2-3 minutes in a 1:1 ratio (10 µl cells: 10 µl Trypan blue) in a microtube. Then,

10 µl of the stained cells was transferred to a counting slide (Bio-Rad) and counted using an automated cell counter (Bio-Rad TC20).

2.1.3. Flow cytometry

Flow cytometry is a laser-based technology used for characterizing cell populations in single cell suspensions. Measured parameters include a cell's relative size and granularity, as well as quantitation of cell surface and intracellular marker expression using fluorochrome-conjugated antibodies. In this research project, a FACSJazz flow cytometer (Becton-Dickinson) was used and the collected data analyzed using FlowJo software (v10.1r5.OSX, FlowJo).

2.1.3.1 Analysis of activated T-cells

Activation with plate-bound anti-human CD3 antibodies plus IL-2 was compared with two other methods of activation: 1) activation with both anti-human CD3 and anti-human CD28 antibodies plus IL-2 and 2) activation with Dynabeads and IL-2 to identify the technique yielding the highest number of activated T-cells before infection with SeV. In one set of experiments, 5 x 10^5 PBMCs obtained from one donor were stimulated in wells of a 24-well plate (Corning) with plate-bound anti-human CD3 antibodies (10 µg/ml, eBioscience) in 500 µl T-cell medium [RPMI (Lonza) containing 10% FBS (Life Technologies) and 175 U/ml IL-2 (Peprotech)], while another 5 x 10^5 PBMCs from the same donor were stimulated instead with plate-bound anti-human CD3 antibodies and anti-human CD28 antibodies (2 µg/ml, eBioscience) in 500 µl T-cell medium [RPMI, 10% FBS, and 30U/ml IL-2].

In the second set of experiments, 5 x 10^5 PBMCs obtained from the same donor as the first set of experiments were stimulated with plate-bound anti-human CD3 antibodies plus 175 U/ml IL-2 in 500ul T-cell medium, while another 5 x 10^5 PBMCs were stimulated instead with 5 µl /well Dynabeads human T-Activator (Life Technologies) and 30 U/ml IL-2 (Peprotech) in 500 µl T-cell medium.

On day 5 after activation, the cells were analyzed for their levels of expression of CD3 (T-cell marker) and CD25 (activation marker) using a FACSJazz flow cytometer (see

Section 2.1.3). In preparation for flow cytometry measurements, four samples were prepared for each technique. For each sample, 5 x 10^5 cells were transferred to 5 ml polypropylene tubes (BD Biosciences) and washed twice with 3 ml PBS (Life Technologies). Three positive samples were prepared: one sample was stained with 5 µl anti-human CD3 conjugated with Phycoerythin-Cyanine [7(PE-Cy7] (BD-Bioscience) only, another sample was stained with 5 µl anti-human CD25-conjugated with Phycoerythin [PE] (BD-Bioscience), and the third sample was stained with 5 µl each of both antibodies. As a negative control, a tube of cells without antibodies was prepared. The samples were incubated on ice for 30 minutes in a 4^{o}C refrigerator, washed two times with 3 ml PBS and then re-suspended in 1 ml PBS for flow cytometry. A blue laser (488 nm) was used for fluorophore excitation with a bandpass filter (585 $\pm$ 29 nm) for CD25-PE and a long pass filter (750/LP) for CD3-PE-Cy7. To eliminate false signals that can result from spectral overlap between the two fluorescent dyed antibodies, readings were done first on the negative control and the two single stained samples. After compensation, data acquisition was carried out on all samples with the limit of 50,000 live cells recording event.

2.1.4. Mitomycin C treatment of mouse embryonic fibroblasts

To support the growth of hiPSCs, mitotically inactivated mouse embryonic fibroblasts (MEF) cells were used as feeder cells. To prepare mitotically inactivated MEFS, 10^6 MEFs (GlobalStem) were plated in a T75 vented-flask (BD Bioscience) in 15 ml MEF medium [ES-DMEM medium (GlobalStem) with 15% FBS (Life Technologies)] and passaged to passage 3 (P3). When the cells reached confluence, 0.5 mg/ml Mitomycin C (Sigma) was added to the MEF medium to yield a final concentration of 10 µg/ml. Inactivation of the expanded MEFs was then carried out according to the manufacturer's (GlobalStem) protocol. Table 2.1 lists the coating conditions and cell densities of the inactivated MEF cells for the 6-well and 12-well plates (Corning) that were used in this research project. 6-well plates were coated with 1 ml 0.1% gelatin in dH_2O (Sigma) and incubated for 1 hour at 37°C prior to seeding the inactivated MEFs. Before seeding, the gelatin was aspirated from the wells. 4 x 10^5 MEFs in 2 ml MEF medium were then seeded into the wells of the 6-well plate.1.5 x 10^5 MEFs in 1 ml MEF medium were seeded into wells in a 12-well plate which was not gelatin coated.

Table 2.1 Inactivated mouse embryonic fibroblasts (MEF) culture conditions

Plate size	Coat	Cell density	Experiment
6-well plate	Gelatin coated	4×10^5	2.1.5
12-well plate	No coat	1.5×10^5	2.1.6

2.1.5. The reprogramming of T-cells

2.1.5.1 Infection with Sendai virus

Activated T-cells, at a density of 5×10^5 cells/ml in T-cell medium [RPMI (Lonza) containing 10% FBS (Life Technologies) and 175 U/ml IL-2], were used for reprogramming. The T-cell infection was performed on day 4 following their activation using temperature-sensitive SeV (CytoTune – iPS 2.0 Sendai Reprogramming Kit, DNAVEC) with a multiplicity of infection (MOI) of 5,5,3 (KOS MOI=5, hc-Myc MOI=5, hKlf4 MOI=3) in T-cell medium. Infection of the activated T-cells with SeV was carried out according to the manufacturer's instructions. 24 hours later, the infected cells were spun down at 800 rpm for 5 min and re-suspended in 2 ml ES medium [Primate ES cell Medium (Reprocell) supplemented with 5 ng/ml bFGF (Invitrogen)] and 10 μM Rho (STEMCELL Technologies), plated on a prepared, one-day old, MEF-coated 6-well plate (see Section 2.1.4) and incubated at 37°C. 48 hours after plating, the culture medium was replaced with 1.5 ml fresh ES medium. From this point onwards, Rho was no longer added to the media. Media (ES medium without Rho) was then changed every two days for a period of 10-20 days after infection until hiPSC colonies formed.

2.1.5.2 Transfection with episomal plasmids

Before transfecting the PBMCs with the four reprogramming transcription factors [63], transfection efficiency was first examined by nucleofecting 3 μg eGFP episomal plasmid (Addgene) into 3.5×10^6 freshly isolated PBMCs using the Human T-cell Nucleofector Kit (Lonza) and nucleofector program V-024 on an Amaxa Nucleofector 2b Device (Lonza). For a negative control, 3.5×10^6 freshly isolated PBMCs were nucleofected under the same conditions but without the addition of the episomal plasmid. The cells were then plated in 2 ml X-vivo 10 medium (Lonza) with 5 μl Dynabeads (Life Technologies) on a 24 hour pre-incubated 6-well gelatin-MEF coated plate (see Section 2.1.4). The expression of eGFP protein was measured 48 hours after nucleofection using a FACSJazz flow

cytometer (Becton-Dickinson). Cells from each well were individually transferred to 5 ml polypropylene tubes (BD Biosciences) and washed twice with 3 ml PBS (Life Technologies) prior to flow cytometry. The eGFP transfection experiment was repeated twice, yielding transfection efficiencies between 18%-24%. The same nucleofection parameters were then used for transfecting PBMCs with the four reprogramming transcription factors.

24 hours before reprogramming, one 6-well plate was coated with 1 ml 0.1% gelatin in dH_2O (Sigma) per well and incubated for 1 hour at 37°C. After aspiration of the gelatin, inactivated MEFs at a density of ~4 x 10^5 per well, were seeded in 2 ml MEF medium [ES-DMEM medium (GlobalStem) with 15% FBS (Life Technologies)] into the wells and the plate incubated in 37°C overnight. On the day of reprogramming, 3 µg total of the reprogramming plasmids [(0.83 µg pCXLE-hOct4-shp53-F, 0.83 µg pCXLE-hSK, 0.83 µg pCXLE-hUL, 0.5 µg pCXWB-EBNA1) (Addgene)] were electroporated into 3.5 x 10^6 PBMCs with the Amaxa Nucleofector 2b Device using the Human T-cell Nucleofector kit according to the manufacturer's instructions. The pre-stored program V-024 for unstimulated human T-cells was used to perform the nucleofection. The electroporated cells were then plated on a one-day-old 6-well MEF-coated plate; approximately 300 µl volume containing a total of 1.1 x 10^6 cells was added to each well, along with 2 ml X-vivo 10 medium and 5 µl Dynabeads. The plate was returned to a 37°C incubator. On days 2 and 4 following electroporation, 1.5 ml ES Medium [Primate ES cell Medium (Reprocell) supplemented with 5 ng/ml bFGF (Invitrogen)] and 10 µM Rho (STEMCELL Technologies) was added to each well without aspiration of the previous medium. On day 6 when the transfected cells, viewed under a phase contrast microscope, were seen to be 90% confluent, the culture medium was replaced with fresh 1.5 ml ES medium supplemented with 10 µM Rho. From day 6, the medium was replaced with fresh ES medium supplemented with Rho as described, every two days for a period of 20-30 days until hiPSC colonies formed.

2.1.6. Maintenance of hiPSCs

2.1.6.1 Feeder-dependent step

Approximately 20-30 days following transfection for the episomal reprogramming system and 10-20 days following infection for the SeV reprogramming system, the resultant individual hiPSC colonies were observed under a phase-contrast microscope and, in a Class II biosafety cabinet, were transferred aseptically using a 10 µl pipette to wells in a 96-well plate. The colonies were further broken up into smaller cell clumps by pipetting gently up and down and then transferred to a prepared MEF-coated 12-well plate, less than 3 days old, containing 1 ml ES medium [Primate ES cell Medium (Reprocell) supplemented with 5 ng/ml bFGF (Invitrogen)] and 10 µM Rho (STEMCELL Technologies). The plated cell clumps were incubated at 37^{o}C. The ES medium without Rho was changed every day until the colony clumps became confluent, as judged visually under a phase contrast microscope. After 5-6 days, 1 mg/ml collagenase type IV (STEMCELL Technologies) was added to each well containing the iPSCs, and incubated for an hour at 37^{o}C until the iPSCs detached from the MEF feeder cell layer.

After 1hour incubation with collagenase type IV, the detached colonies were spun down in ES medium for 5 min in 1,000 rpm. Then the cell pellet was broken with 2 ml mTeSR1 medium (STEMCELL Technologies) supplemented with 10 µM Rho, and transferred to the 0.5 mg/well Matrigel (Corning) in DMEM/F12 (Life Technologies) coated wells of a previously prepared 6-well plate and returned to a 37^{o}C incubator.

2.1.6.2 Feeder free step

The mTeSR1 medium was changed daily in the 6-well plates described in Section 2.1.6.1 until the colonies became confluent. After adherence of the iPSCs to the surface of the Matrigel-coated 6-well plate but before they became confluent, MEF cells, which were originally transferred with the hiPSCs during the feeder dependent step, were physically removed using 10 µl pipette tips under a phase contrast microscope. The hiPSCs were then allowed to continue growing until they became confluent when viewed under a phase contrast microscope. At that point, the medium was aspirated and 1 ml 0.02% EDTA (Lonza) was added to each well. The colonies and EDTA were incubated for 5-10 minutes at room temperature. The EDTA was then aspirated and 2 ml mTeSR1

medium supplemented with 10 μM Rho was added to each well. The medium was pipetted up and down several times to detach the cells from the surface of the wells. Once detached and re-suspended in the mTeSR1 medium with 10 μM Rho, each cell line was divided into two new wells of a Matrigel coated 6-well plate. The mTeSR1 medium was changed every day until the cells became confluent whereupon the process of detachment (the next passage) was repeated.

2.1.7. Cryopreservation of hiPSCs

hiPSC colonies at the feeder-free step were cryopreserved for future experiments using STEM-CELLBANKER cell freezing media (amsbio, Oxford UK) and following the manufacturer's instructions. Cell lines from later passages were also frozen in the same manner and stored first for 24 hours at -80°C and then transferred to a nitrogen tank at -160°C for longer-term storage.

2.1.8. Characterization of hiPSCs for pluripotency

2.1.8.1 Immunocytochemistry of live cells

One well of newly generated colonies from each donor was used for live staining for CD44 (differentiation marker) and TRA-1-60 (pluripotency marker). Live staining of the iPSC colonies was carried out using Stem Cell Antibody Kits for Live Cell Imaging (Life Technologies) following the manufacturer's instructions. Stained colonies were imaged using a Nikon Epi-fluorescence microscope and 400 two-dimensional snapshots, using 20x objectives (1661 μm x 1404 μm in the X and Y planes, respectively), were taken of the contents of each well. The snapshots were then stitched together and visualized using ImageJ software (ImageJ).

To complement the live staining results, the iPSC induction efficiency was calculated based on the number of iPSC colonies per number of seeded cells, which were estimated from the number of cells used for nucleofection and SeV infection.

2.1.8.2 Flow cytometry analysis of pluripotent surface markers

iPSCs generated on passage 5 (1 time passage on MEF and 4 times passage on Matrigel) were characterized for two pluripotency surface markers, stage-specific embryonic antigens -4 (SSEA-4) and TRA-1-60, using a FACSJazz flow cytometer (Becton-Dickinson). The medium for each cell line was aspirated from two confluent wells of colonies and 1 ml dissociation solution (0.02% EDTA; Lonza) was added to each well. The colonies and EDTA were incubated for 5-10 minutes at room temperature. The EDTA was then aspirated and 2.5 ml mTeSR1 medium (STEMCELL Technologies) added to each well, with pipetting up and down several times to detach the cells from the surface of the well. Cells from two wells of the 6-well plate (the same cell line) were then divided equally into five 5 ml polypropylene tubes (BD Biosciences) and washed twice with 3 ml PBS (Life Technologies). Each cell line experiment had two negative controls and three positive controls. One positive control was stained for two monoclonal antibodies; 5 µl Alexa Flour 647 Mouse anti-Human TRA-1-60 Antigen (BD Bioscience) and 20 µl PE Mouse anti SSEA-4 (BD Bioscience), according to the manufacturer's instructions while the other two positive controls were stained with only one of the two antibodies. One negative control remained unstained (to identify background noise) and the second negative control was stained with isotypes of the two antibodies (to detect any nonspecific binding [false positive]). A blue laser (488 nm) with an excitation band pass filter of 585 $\pm$ 29 nm was used for SSEA-4 PE while a red laser (640 nm) with an excitation band pass filter of 670 $\pm$ 30 nm was used for TRA-1-60 AlexaFluor647. Cell lines found to have higher expression levels of these two markers were passaged five more times and on passage 10 (1 time passage on MEF and 9 times passage on Matrigel) were characterized again for expression of TRA-1-60 and SSEA-4 using the same protocol.

2.1.8.3 hiPSC RNA extraction, qRT-PCR

RNA from hiPSCs collected on passages 5 and 10 was extracted according to the manufacturer's instructions using the RNeasy Mini Kit (QIAGEN). The concentrations of the extracted RNA were measured using a NanoDrop Spectrophotometer ND-1000 (NanoDrop) at wavelength ratio of 260 / 280 nm and the RNA was then stored at -80^{o}C for later analysis.

1 µg from each extracted RNA sample was reverse transcribed into cDNA using the QuantiTect Reverse Transcription Kit (QIAGEN) according to the manufacturer's instructions. The concentration of generated cDNA was measured using a NanoDrop Spectrophotometer ND-1000 and the concentration of cDNA was then adjusted to 2 ng/µl through serial dilution with RNAse free water (Qiagen). The master mixes contained 10 µl SYBR Select Master mix for CFX (Life Technologies) and for each pluripotent gene (Sox-2, Oct4, c-Myc, Klf4, Nanog and ZFP-42) 2 µl of forward primer and 2 µl of reverse primer (Integrated DNA Technologies, see Appendix B for primer sequences) with a final concentration of 2.5 µM each and 1 µl of RNase-free water. 10 ng (5 µl) cDNA was added to the reaction for a final reaction volume of 20 µl. Two negative controls were used for each pluripotent gene: one control did not contain cDNA while the other control contained cDNA from the donor's activated T-cells. The thermal cycling protocol applied for the qRT-PCR was as follows: 1) initial activation step of 3 min at 95°C; 2) 3-step cycling including: a) denaturation for 10 secs at 95°C; b) annealing for 40 secs at 60°C; c) extension for 5 secs at 65°C (these three steps were repeated for 39 cycles); and 3) end of PCR cycling held at 4°C.

2.1.9. *In vitro* cardiac differentiation of hiPSCs

After analyzing the generated hiPSCs for the expression of two surface markers, SSEA-4 and TRA-1-60, on passage 10 (as described in Section 2.1.8.2), the hiPSCs that expressed both of these markers were chosen for cardiac differentiation. After the medium was removed, the generated hiPSCs were detached from Matrigel-coated wells in a 6-well plate by adding 1 ml 0.02% EDTA (Lonza) to each well. The colonies and EDTA were incubated for 5-10 minutes at room temperature, following which the EDTA was aspirated and 2 ml mTeSR1 medium supplemented with 10 µM Rho was added to each well. The medium was pipetted up and down several times to detach the cells from the surface of the wells. Once detached and re-suspended in the mTeSR1 medium with 10 µM Rho, the cells were counted using an automated cell counter (Bio-Rad TC20) (see Section 2.1.2 for protocol). 1 x 10^6 cells from each cell line were then seeded on 6 well Matrigel-coated plates and 2 ml mTeSR1 medium supplemented with 10 µM Rho was added to each well. The mTeSR1 medium was changed every day until the cells became confluent. When cells became almost 100% confluent after viewing under phase-contrast microscope, the

differentiation pathway was initiated, following Lian et al's protocol[116]. The differentiation protocol was optimized and performed by Sanam Shafaattalab, a PhD candidate in our laboratory.

2.1.10. CM RNA extraction, qRT-PCR

The protocol for qRT-PCR to analyze cardiac gene expression is the same as the protocol described in Section 2.1.8.3 for hiPSCs, except that cardiac markers, adult and fetal isoforms of TNT2, TNI 3 (cardiac isoform), TNI 1 (skeletal isoform), and myosin light chain-2 (atrial and ventricular paralogs) were used instead of Sox-2, Oct4, c-Myc, Klf4, Nanog and ZFP-42. See Appendix B for the CM primer sequences. Two negative controls were used for each pluripotent gene: one control did not contain cDNA while the other control contained cDNA from the iPSC cell line from which the CMs were derived.

Chapter 3. Results

3.1.1. Isolated PBMC count

The yield and percentage viability of the harvested PBMCs from each individual donor was determined after isolation, staining with Trypan blue (Lonza) and counting using an automated cell counter (Bio-Rad TC20) (see Section 2.1.2 for protocol). The total number of isolated PBMCs from 1 ml of each donor's whole blood was between 1.5 x 10^6 cells and 2 x 10^6 cells; the percentage of viable (actively growing and dividing) cells in the total counted cells for each donor was 87%-92%.

3.1.2. Trypan blue exclusion assay results

Three separate blood samples were taken from one donor, following which the T-cells in 5 x 10^5 PBMCs from each sample (series 1, 2, and 3) were selectively activated using CD3-plate bound antibodies and IL-2. Staining the cells with Trypan blue, the total number of cells and the number of viable cells were then counted in the Bio-Rad TC20 cell counter, as described in Section 2.1.2, every day over a period of one week. In all three series, in days 1 and 2 following activation, between 10-20% of the total number of cells were found to have died but the percentage of viable cells began to increase after days 2 and 3. Also within all three series, a 20% increase in the number of viable cells was observed from days 3 to 5. In series 1 and 2, after days 5 and 6, the percentage of viable cells was found to have decreased by 20-30% but increased in series 3, remaining in log phase.

The percentage of viable cells in each series was calculated using the following equation:

$$\%\ of\ viable\ cells = \left(\frac{Total\ Number\ of\ viable\ cells}{Total\ Number\ of\ viable\ and\ non-viable\ cells}\right) \times 100$$

and is shown graphically in Figure 3.1:

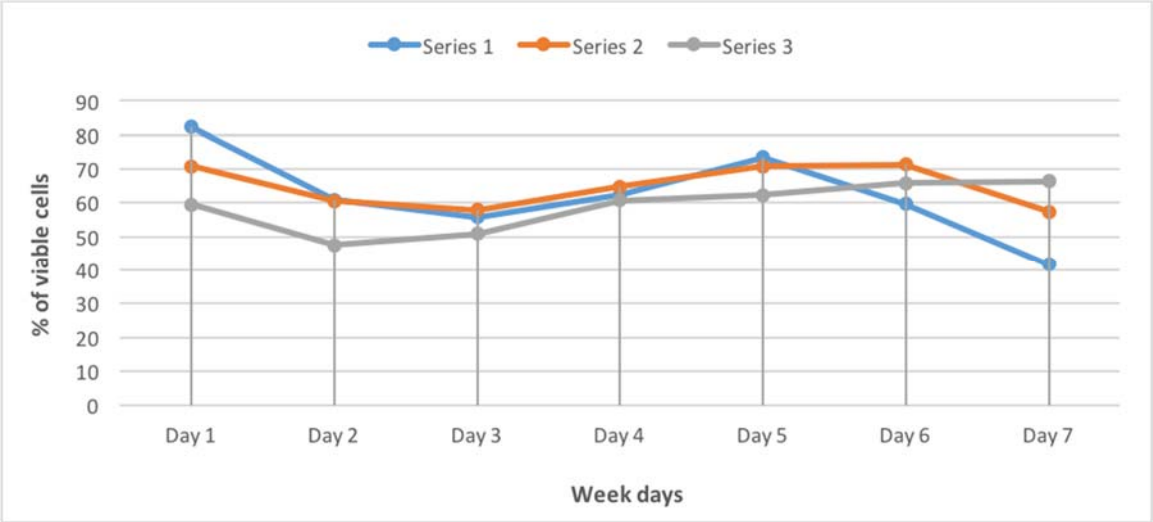

Figure 3.1 The percentage of viable cells within total cell populations.
Three separate blood drawings were taken from one donor and from each sample, 5 x 10^5 PBMCs were isolated. The T-cells in each sample (series 1, 2, and 3) were selectively activated using CD3-plate bound antibodies and IL-2. Cells in each series were counted every day for one week. Between 10%-20% of the total number of cells observed from day 1 to day 2 after activation died but the percentage of viable cells began to increase after days 2 and 3. A 20% increase in viable cells was observed from days 3 to 5 for each series. After days 5 and 6, the percentage of viable cells decreased by 20%-30% in series 1 and 2 but increased, remaining in the log phase of growth, in series 3.

3.1.3. Results from flow cytometry analysis of activated T-cells

Activation of T-cells within a PBMC population is required for downstream SeV transduction. To determine the time frame in which the numbers of activated T-cells begin to increase and reach maximum population, four sets of experiments stimulating PBMCs derived from one donor using the anti-CD3 antibodies and IL-2 protocol described in Section 2.1.1 were performed. In all four sets, the percentage of cells positively stained for both T-cell and activation markers were measured daily for a period of one week. Five days after activation, the maximum percentage of activated T-cells (between 93%-97%) was measured. This level was maintained on day 6 and started to decrease slightly on day 7.

Knowing the timeline to maximally activated T-cell numbers; the next step was to identify the most effective and efficient method of T-cell activation. Three different protocols were carried out on blood drawn from one donor, as described in Section 2.1.1.

In the first series of experiments, the T-cell activation procedure using anti-CD3 antibodies and IL-2 (Figure 3.2.a), as was done on the timeline experiments, was compared to the Dynabeads and IL-2 method (Figure 3.2.b). The percentage of activated T-cells on day 5 following activation was determined using flow cytometry. In the second set of experiments, T-cell activation with anti-CD3 antibodies and IL-2 (Figure 3.2.c) was compared to activation with anti-CD3 and anti-CD28 antibodies plus IL-2 (Figure 3.2.d) on day 6 post activation. Due to facility limitations, flow cytometry was delayed by one day for the second set of experiments.

In the first set of experiments, 93% of PBMCs stimulated using the anti-CD3 antibodies plus IL-2 method were found to be positive for both activation and T-cell markers while only 82% were found to be positive in the Dynabeads plus IL-2 protocol, 5 days after activation. In the second set of experiments, 75% of the PBMCs stimulated with anti-CD3 antibodies plus IL-2 were positive for both activation and T-cell markers while only 46% were positive in the anti-CD3 and anti-CD28 antibodies plus IL-2 method 6 days following activation. The highest percentage of activated T-cells was seen in the anti-CD3 antibody and IL-2 protocol 5 days post activation, which correlates with the observation in Section 2.3.1 that the percentage of viable cells began to decrease 5 days after activation.

In both sets of experiments, the anti-CD3 antibodies plus IL-2 protocol yielded higher percentages of activated T-cells than either the Dynabeads plus IL-2 protocol or the anti-CD3 and anti-CD28 antibodies plus IL-2 procedure. As a result, the anti-CD3 antibodies plus IL-2 method was selected as the T-cell activation protocol to be used before SeV reprogramming.

Although the anti-CD3 antibodies plus IL-2 protocol is best for the SeV reprogramming system, it is not for the episomal system. Results in Section 3.1.6 demonstrated that electroporation of activated T-cells is not efficient while isolation and expansion of T-cells after electroporation using Dynabeads was (Section 3.1.6 likely due to effective interaction of the mobilized Dynabeads with the T-cells, stimulating their activation[63,85].

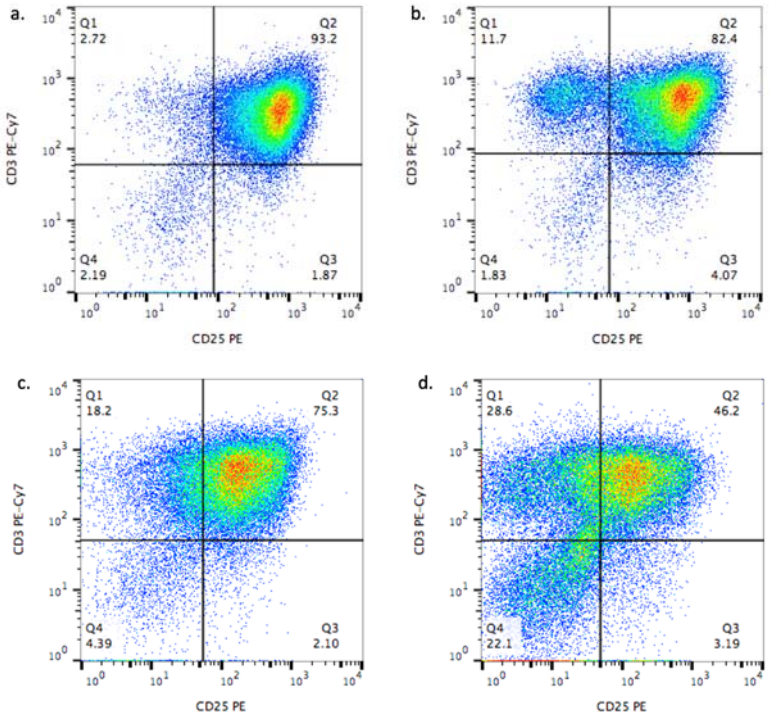

Figure 3.2 Flow cytometry analysis of activated T-cells with three different activation protocols on blood drawn from one donor in two sets of experiments.

Stimulated cells were stained with PE-Cy7-labelled anti-human CD3 antibodies (which bind to the CD3 antigen on the surface of T-cells) and PE-labelled anti-human CD25 antibodies (which bind to the CD25 antigen on the surface of activated T-cells) as described in Section 2.1.3.1. (a) 93% of PBMCs stimulated with anti-CD3 antibodies and IL-2 were positive for both activation and T-cell markers 5 days post activation while, (b) 82% of PBMCs stimulated with Dynabeads and IL-2 were positive for both activation and T-cell markers after 5 days. (c) 75% of PBMCs stimulated with anti-CD3 antibodies and IL-2 were positive for both activation and T-cell markers 6 days post activation and, (d) 46% of PBMCs stimulated with anti-CD3 and anti-CD28 antibodies plus IL-2 were positive for both activation and T-cell markers 6 days following activation.

3.1.4. Activated T-cell morphology results

Phase contrast images were taken of PBMCs 24 hours following activation with anti-CD3 antibodies and IL-2 and on day 5 post activation. A hallmark of activated T-cells is aggregation and this was observed by day 5, as shown in Figure 3.3. These visual results correlate with the flow cytometry results, confirming the presence of activated T-cells within the expanded population of viable cells counted in the Trypan blue assays.

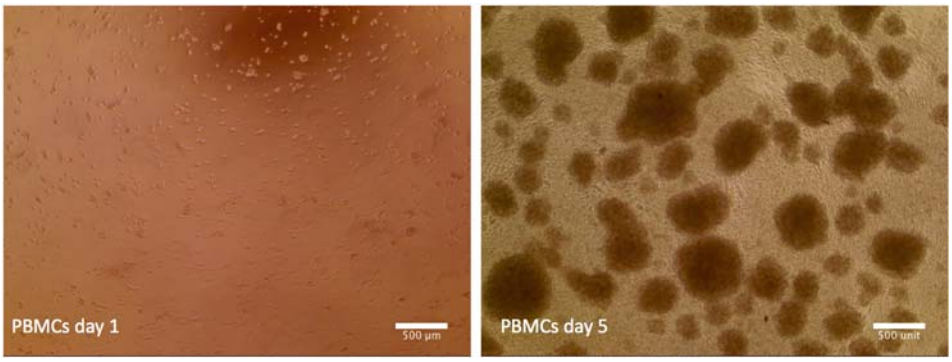

Figure 3.3 Activation of PBMCs with anti-CD3 antibodies and IL-2 induces T-cell aggregation.

These two phase-contrast images are PBMCs activated with 10 µg/ml anti-CD3 antibodies and 175 U/ml IL-2. The day 1 image was taken 24 hrs. after activation and the image of PBMCs on day 5 was taken ~120 hrs. after activation. The images show that the T-cell subpopulation aggregates after activation with anti-CD3 antibodies and IL-2.

3.1.5. Results of MEF feeder cell density optimization

As described in Sections 2.1.4, MEF cells were seeded in different densities (3 x 10^5 cells/well, 3.5 x 10^5 cells/well, 4 x 10^5 cells/well, 5 x 10^5 cells/well and 7 x 10^5 cells/well) on gelatin coated 6-well plates for a period of 9 days under transfection conditions, excluding transfected cells. Of these densities, MEF cells on gelatin coated plates with a density of 4 x 10^5 cells/well maintained the appropriate confluency of 70-80% after 9 days; not too sparse to be insufficient to support pluripotent stem cells and not too confluent to detach spontaneously after being cultured for that length of time. For wells with initial cell densities of 3 x 10^5 cells/well and 3.5 x 10^5 cells/well, confluency decreased to 40-50% after 9 days culturing and for wells with initial cell densities of 5 x 10^5 cells/well and 7 x 10^5 cells/well, although confluency was comparable with 4 x 10^5 cells/well after 9 days, the number of detached and floating cells increased steeply.

Once the appropriate cell density (4 x 10^5 cells/well) was determined for MEFs on gelatin-coated plates, the same density was then plated on non-coated 6-well plates. After being cultured for 9 days, the cells were only 20-30% confluent; too sparse to support hiPSC growth. MEF cells with a density of 4 x 10^5 cells/well on gelatin coated 6 well plates were demonstrated to be the optimal density and condition for successful growth of hiPSCs.

3.1.6. Results of optimization of nucleofection in the episomal reprogramming system

3 μg of eGFP-episomal plasmids were nucleofected into both activated T-cells and unstimulated PBMCs as described in Section 2.1.5.2. Flow cytometry analysis of eGFP expression 48 hours post transfection revealed successful transfection of eGFP plasmids occurred in unstimulated PBMCs but not in activated T-cells. The transfection efficiency (percentage of cells expressing eGFP) was 24% in PBMCs derived from fresh human blood and 14% and 17% in PBMCs derived from frozen human blood (donated by Dr. Jonathan Choy, Molecular Biology and Biochemistry Department, Simon Fraser University).

3.1.7. HiPSC morphology results

Phase contrast images were taken of hiPSCs generated by either the SeV reprogramming system or the episomal reprogramming system, following two passaging on MEFs (see Figure 3.4). As viewed through the 4X objective lens, undifferentiated colonies of small, round hiPSCs were the result in both reprogramming systems while through the 20X objective lens, the large nuclei in individual cells could be seen. This is characteristic of highly mitotically active cells and is a signature of pluripotent stem cells.

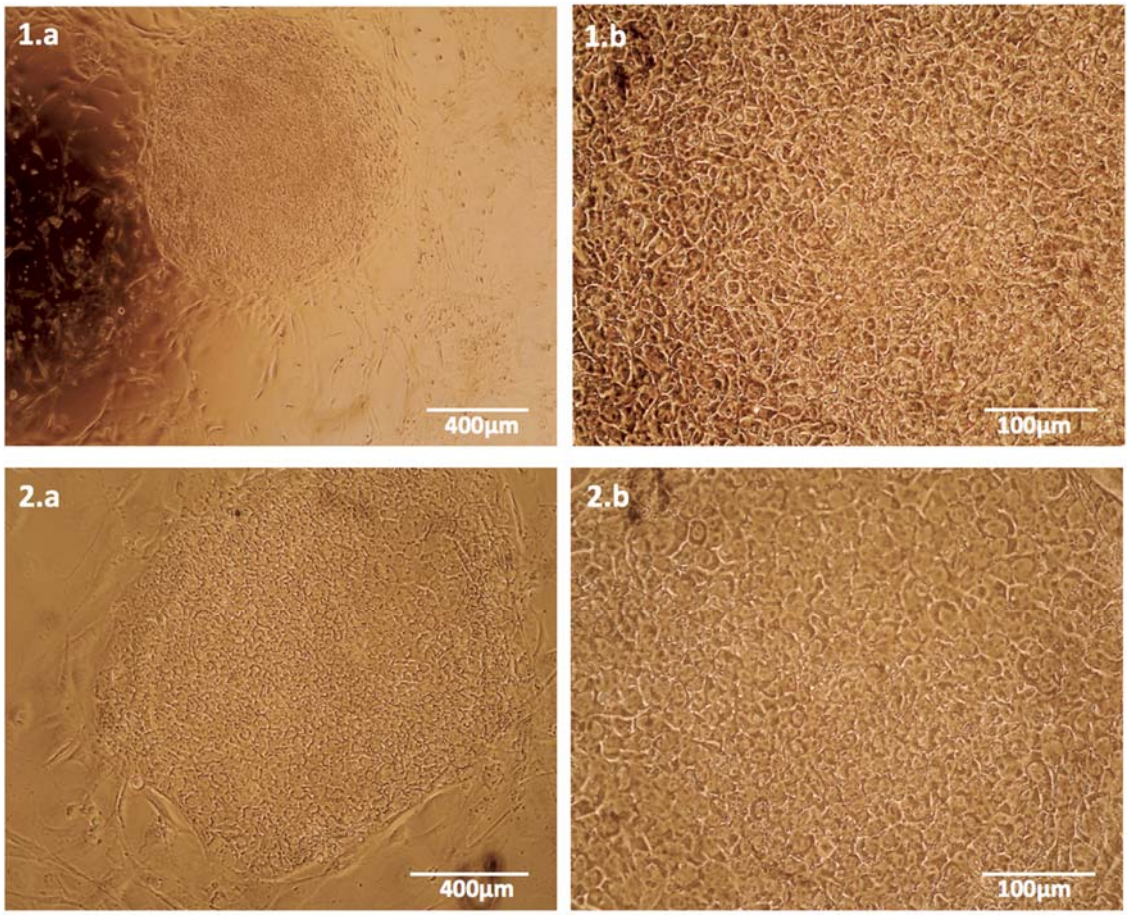

Figure 3.4 Morphology of hiPSCs generated by both reprogramming systems following two passages on MEFs.

Seen under a phase contrast light microscope, the hiPSCs in images 1 (a) and (b) were generated using the SeV reprogramming system while hiPSCs in images 2 (a) and (b) were generated using the episomal reprogramming system. Images 1 (a) and 2 (a) viewed through a 4x objective lens, show undifferentiated hiPSC colonies of small, round cells, clearly separate from the feeder layer cells. Images 1 (b) and 2 (b), magnified by a 20x objective lens, show hiPSCs with large nuclei.

3.1.8. Immunocytochemistry results from live cell staining

A combination of two antibodies, one against TRA-1-60 (a stem cell surface marker) conjugated with Alexa Fluor555 and another against CD44 (a differentiated cell marker) conjugated with Alexa Fluor488, was used to live stain the primary generated hiPSCs (the first colonies obtained from the reprogramming of activated T-cells), as described in Section 2.1.8.1. Figure 3.5 shows hiPSCs derived from both the SeV and episomal reprogramming systems. Pluripotent cells, in each colony, that expressed the TRA-1-60 surface marker are coloured red while the MEF cells the hiPSCs are growing

on are coloured green. This test confirmed that both reprogramming systems generated hiPSCs.

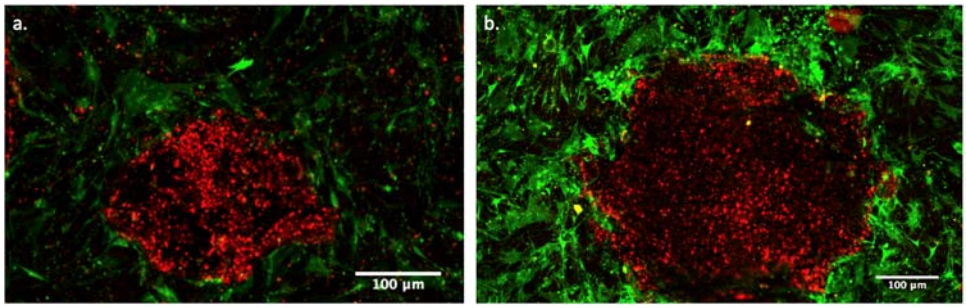

Figure 3.5 Epifluorescent imaging of single primary hiPSC colonies generated from the SeV and episomal reprogramming systems.

The epifluorescent image (a) is of a single hiPSC colony generated from SeV reprogramming while image (b) is of a single hiPSC colony generated from episomal reprogramming. Both hiPSC colonies were derived from the same donor's blood samples.

3.1.8.1 Comparison of the efficiency of the SeV and episomal reprogramming systems in Donor 002 hiPSCs

400 two-dimensional snapshots were taken of hiPSCs generated from the blood sample of Donor 002 using either the SeV or episomal reprogramming systems in wells of a 6-well plate. The snapshots were then stitched together, as described in Section 2.1.8.1. Cells stained for the presence of the differentiated cell marker, CD44, were pseudo-coloured green while cells stained for the presence of the stem cell surface marker, TRA-1-60, were pseudo-coloured red.

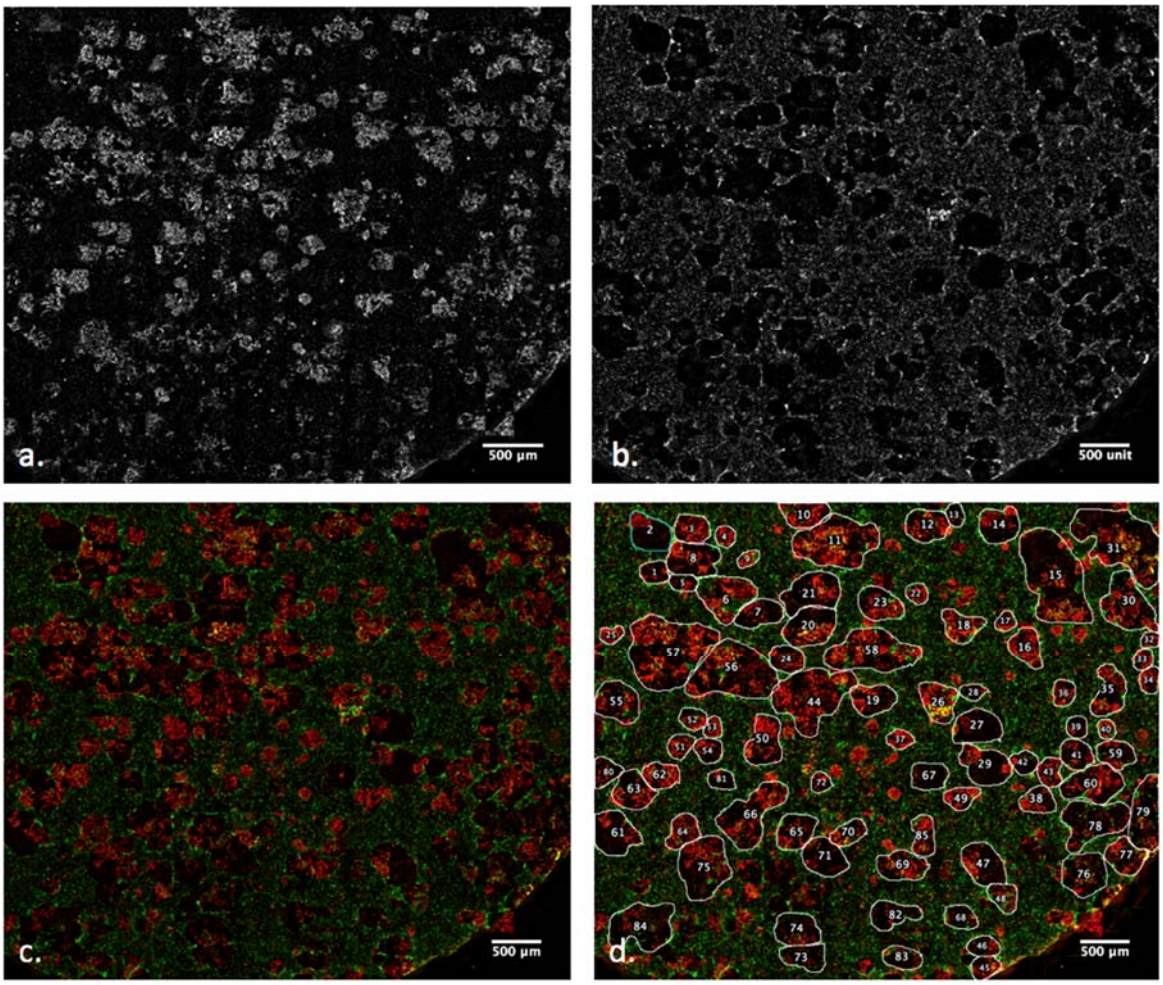

Figure 3.6 Epi-fluorescent imaging of primary hiPSCs generated from SeV reprogramming of PBMCs derived from Donor 002.

The epi-fluorescent image (a) shows the hiPSCs in grey scale while in image (b) the feeder layer is shown in grey scale and the black holes are the hiPSC colonies. After applying two pseudo-colours, image (c) is the result. hiPSCs are shown in red and feeder layer and differentiated cells are coloured green. In image (d) hiSPC colonies were manually outlined and individually numbered. The area of the smallest selected colony was 25,263 μm^2 and the area of the largest colony was 187,136 μm^2. By comparing image (d) with image (b), the smaller red spots were determined to be background noise. A total of 87 colonies were counted.

Figure 3.6 shows the same image of hiPSCs generated from the SeV reprogramming system, first in grey scale and then in pseudo-colour, with the hiPSCs coloured red, indicating the presence of TRA-1-60, and the feeder layer and differentiated cells coloured green, indicating the presence of CD44. The area of the smallest hiPSC colony was 25,263 μm^2 and the largest colony's area was 187,136 μm^2. Twenty out of the 87 colonies revealed the presence of both pluripotent and differentiation markers,

indicating overgrowth of the colonies. Colony overgrowth results in spontaneous differentiation of the hiPSCs, which can be evidenced by hypertrophic colonies, colonies without borders and flattened cells[117]. In future experiments, the colonies need to be picked 2 to 3 days after formation rather than the 6 days used for these results.

Using the equations below, the efficiency of the SeV reprogramming system in generating hiPSCs was calculated and found to be 0.044%.

$$Efficiency\ of\ SeV\ system\ for\ Donor\ 002 = (\frac{Number\ of\ counted\ colonies}{Number\ of\ seeded\ infected\ cells}) \times 100$$

$$Efficiency\ of\ SeV\ system\ for\ Donor\ 002 = \left(\frac{87}{2 \times 10^5}\right) \times 100 = 0.044\%$$

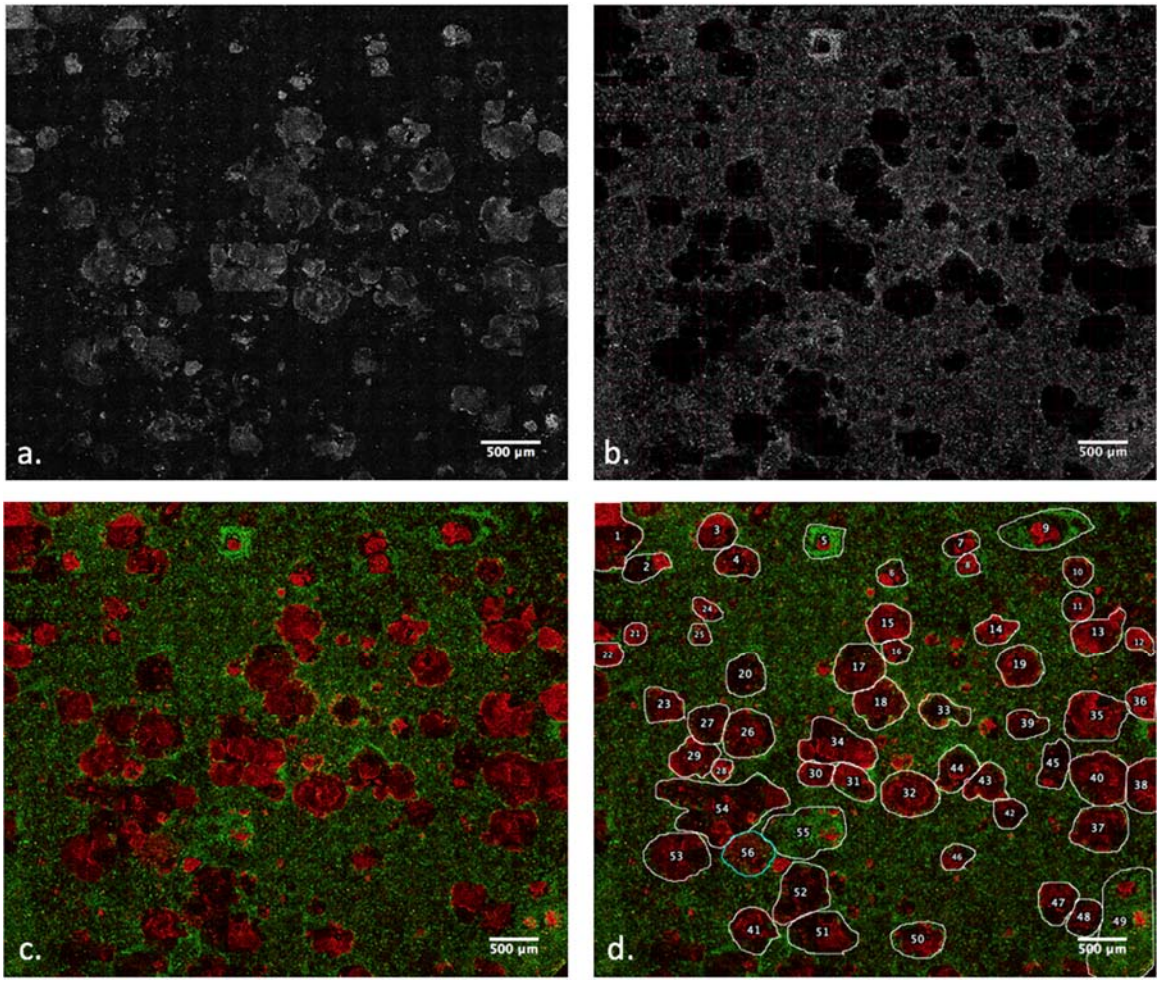

Figure 3.7 Epi-fluorescent imaging of primary hiPSCs generated from episomal reprogramming of PBMCs derived from Donor 002.

Image (a) shows the hiPSCs in grey scale while image (b) shows the feeder layer in grey scale where the black holes are the hiPSC colonies. Image (c) is the same image after applying the two pseudo-colours. hiPSCs show as red and the feeder layer and differentiated cells show as green. In image (d) colonies are outlined manually and individually numbered. The area of the smallest selected colony was 26,488 μm^2. The smaller red spots were identified as background noise by comparing image (d) with image (b). The area of the largest colony was 399,796 μm^2. Four colonies out of 56 expressed both differentiation and pluripotent markers.

Figure 3.7 shows the same image in grey scale and then in pseudo-colour to first identify the hiPSC colonies generated from the episomal reprogramming system using Donor 002's blood sample and then the presence or absence of differentiation and pluripotent markers in specific colonies. Four out of 56 colonies generated through the episomal reprogramming system were found to express both differentiation and pluripotent markers due to overgrowth.

Using the equations below, the efficiency of the episomal reprogramming system in generating transfected hiPSCs was calculated and found to be 0.005%.

$$Efficiency\ of\ episomal\ system\ for\ Donor\ 002 = (\frac{Number\ of\ counted\ colonies}{Number\ of\ seeded\ transfected\ cells}) \times 100$$

$$Efficiency\ of\ episomal\ system\ for\ Donor\ 002 = \left(\frac{56}{1.1 \times 10^6}\right) \times 100 = 0.0051\%$$

Comparing the efficiency of the SeV reprogramming system (0.044%) to the episomal reprogramming system (0.0051%) revealed that the SeV system, using Donor 002's PBMCs, was nine times more efficient than the episomal system.

Figure 3.8 shows the colony sizes and frequency distributions of hiPSCs generated from the SeV and episomal reprogramming systems. For hiPSCs derived from SeV transduction, the colony areas ranged from less than 100,000 μm^2 to 500,000 μm^2 while, for the hiPSCs derived from episomal transfection, the colony areas ranged from less than 100,000 μm^2 to 300,000 μm^2. For hiPSCs from both systems, the majority of the colonies were in the less than 100,000 μm^2 category (51% for the SeV and 59% for the episomal hiPSCs) and the 100,000 μm^2 to 200,000 μm^2 category (36% for both systems). In both systems, the majority of hiPSC colonies had areas less than 100,000 μm^2. Colonies expressing the differentiation marker had areas more than 200,000 μm^2, which correlates with the fact that differentiation increases as colony overgrowth occurs.

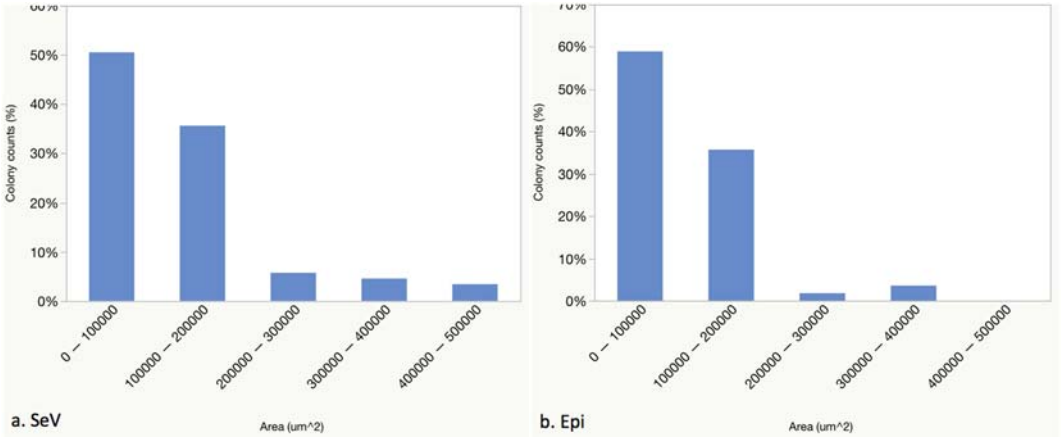

Figure 3.8 Colony size and frequency distributions among hiPSCs generated from SeV and episomal reprogramming systems

All colonies (undifferentiated and partially differentiated) were counted in this experiment. Figure 3.8 (a) represents the size and frequency distribution of hiPSC colonies generated using the SeV reprogramming system. There was a large range of colony areas. 51% of the colonies had area sizes less than 100,000 μm^2; 36% of the colonies had areas between100,000 μm^2 and 200,000 μm^2; 6% had areas between 200,000 μm^2 and 300,000 μm^2; 5% had areas between 300,000 μm^2 and 400,000μm^2; and 3% had areas between 400,000 μm^2 and 500,000 μm^2. Figure 3.8 (b) represents the size and frequency distribution of hiPSC colonies generated from the episomal reprogramming system. The range of colony areas was less than the areas of hiPSCs derived from the SeV system. 59% of the colonies had areas less than 100,000 μm^2; 36% had areas between 100,000 μm^2 and 200,000 μm^2; and 2% had areas between 200,000 μm^2 and 300,000 μm^2. No colonies with an area equal to or greater than 300,000 μm^2 were measured in the episomal reprogramming system hiPSCs.

3.1.9. Flow cytometry analysis of pluripotent surface markers

HiPSCs generated from both the SeV and episomal reprogramming systems were quantified for the expression of two specific pluripotent surface markers (SSEA-4 and TRA-1-60) at two different passages, P5 and P10, as described in Section 2.1.8.2. The percentage of positively stained cells for each marker was estimated for cell lines derived from each reprogramming system, with SSEA-4 coloured red and TRA-1-60 assigned blue. The bar columns, with error bars, in Figure 3.9, represent the mean percentages of positively stained cells for each surface marker at P5 and P10 for each reprogramming system (see Appendix C for more details).

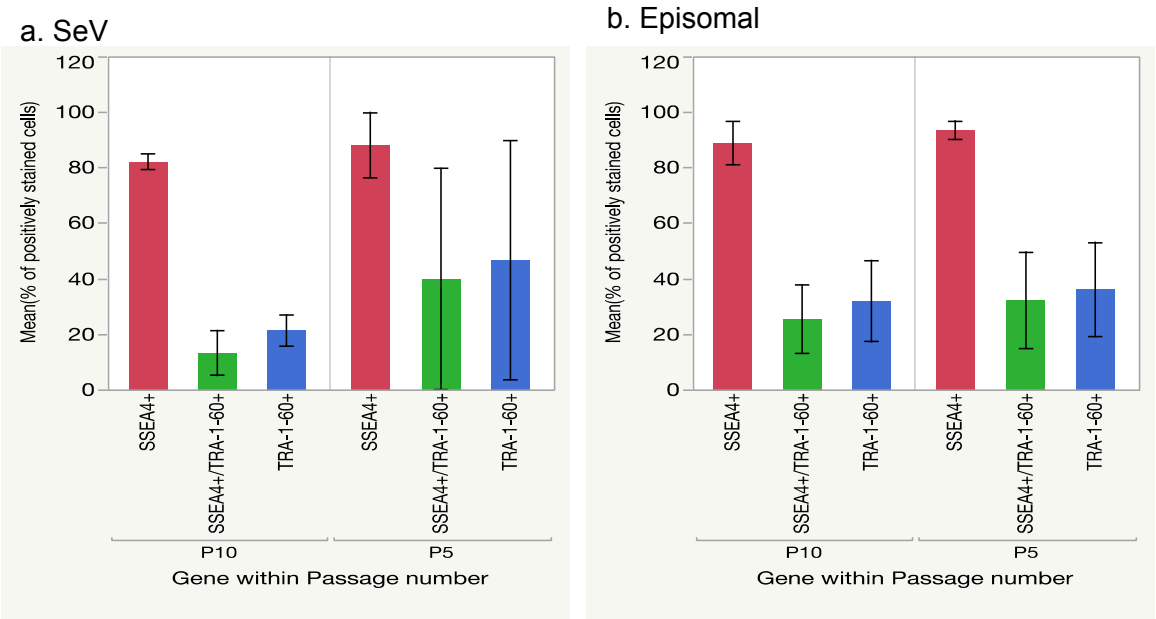

Figure 3.9 Flow cytometry analysis of SeV and episomally generated hiPSCs for the presence of TRA-1-60 and SSEA-4 markers at P5 and P10.

Cell lines in the SeV system (n=3) two from donor Sevii001 and one from donor Sevii002 and in the episomal system (n=7) two from donor Epii001, one from donor Epii002, three from donor Epii003 and one from donor Epii004 were studied at two different passages (P5 and P10). (Error bars shown as ±1 SEM.) In both the SeV and episomal systems, the cell lines did not show a difference in the expression of SSEA-4 between P5 and P10. More than 80% of the cells were positive for SSEA-4 in both reprogramming systems for P5 and P10. The SEM for SSEA-4 was smaller than that for TRA-1-60 in P5 and P10 for both reprogramming systems.

For both the SeV and episomally generated hiPSCs, there was no significant difference in the expression of SSEA-4 in either P5 or P10, with more than 80% of all cells expressing SSEA-4 in both passages. Table 3.1 provides the numerical data. In comparison with SSEA-4, TRA-1-60 was expressed at a lower level by episomally generated hiPSCs in P5 and P10 and by SeV generated hiPSCs in P10. The size of the error bar in the TRA-1-60 result for the SeV generated hiPSCs at P5 was extremely large but indicates that the marker is expressed at levels similar to or lower than that of SSEA-4.

Table 3.1 Pluripotent surface markers in the SeV and Episomal reprogramming systems

	Reprogramming system= Sev				Reprogramming system= Epi			
	SSEA4+		TRA-1-60+		SSEA4+		TRA-1-60+	
Passage#	Mean	SE	Mean	SE	Mean	SE	Mean	SE
P5	88.1	5.9	46.6	21.5	93.4	4.4	36	8.4
P10	82	1.3	21.26	2.8	88.7	3.8	31.8	7.3

3.1.10. qRT-PCR analysis of pluripotent gene expression in hiPSCs at P5 and P10.

qRT-PCR was used to determine the levels of expression of six pluripotent markers-Sox2, Klf4, ZFP-42, Nanog, Oct4, and c-Myc--in hiPSCs generated by the SeV (derived from two donors) and episomal (derived from four donors) reprogramming systems. Cells at passages 5 and 10 were studied. Figure3.10 shows the results in the form of bar graphs, with error bars shown as ± 1 SEM. For the SeV generated hiPSCs, there was no significant difference in OCT-4 expression levels between P5 and P10 which was also true of c-MyC expression. Only one SeV cell line out of three expressed Nanog but in the cell line that expressed Nanog, both Nanog and Oct4 expression levels were higher than c-Myc for passages 5 and 10. Table 3.2 shows the values calculated for the expression levels of each marker.

For the episomally generated hiPSCs, there were no differences between P5 and P10 expression levels of Nanog, Oct4, or c-Myc. However, as with the SeV generated hiPSCs, Nanog and Oct4 were expressed at higher levels than c-Myc at both passages.

Comparing expression levels of these pluripotent markers in hiPSCs generated from both reprogramming systems, Oct4 expression is higher in the SeV generated hiPSCs while c-Myc levels are similar across both systems. Nanog expression levels, while higher than c-Myc levels, are also comparable in both systems.

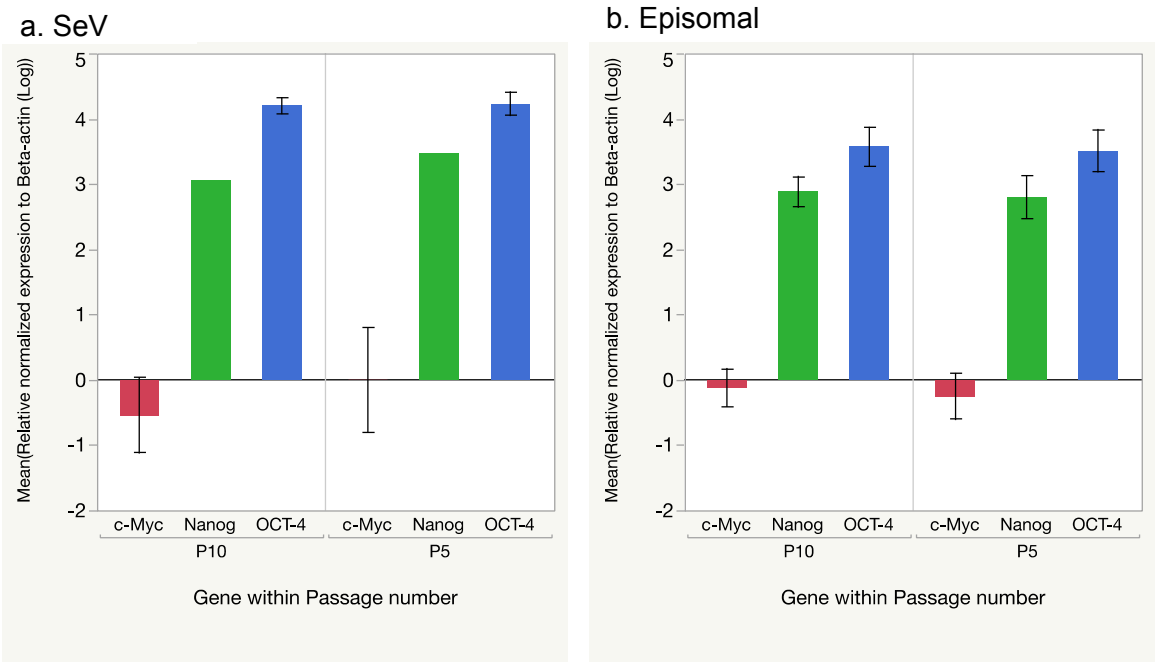

Figure 3.10 qRT-PCR analyses of pluripotent genes in hiPSCs for passages 5 and 10

Cell lines in the SeV system (n=3) two from donor Sevii001 and one from donor Sevii002 and in the episomal system (n=7) two from donor Epii001, one from donor Epii002, three from donor Epii003 and one from donor Epii004 were studied at two different passages (P5 and P10). (Error bars shown as ± 1 SEM.) (a) This bar graph shows the expression levels of three pluripotent genes in hiPSCs generated from the SeV system. Only one cell line out of three expressed Nanog so no standard error was determined for this transcript. (b) The expression levels of the genes in hiPSCs derived from the episomal system are shown in this bar graph.

Table 3.2 Pluripotent endogenous gene expression in the SeV and episomal reprogramming systems

		c-Myc		Nanog		Oct4	
Reprogramming System	Passage#	Mean	SE	Mean	SE	Mean	SE
Sev	P5	-0.002	0.4	N/A	N/A	4.2	0.1
	P10	-0.5	0.3	N/A	N/A	4.2	0.06
Epi	P5	-0.25	0.17	2.8	0.16	3.5	0.16
	P10	-0.12	0.14	2.9	0.12	3.6	0.15

3.1.11. qRT-PCR analysis of cardiac specific gene expression in hiPSC-derived CMs

qRT-PCR was run on hiPSC-derived CMs generated using both the SeV and episomal reprogramming systems to determine the level of expression for cardiac-specific genes. While the error bars are large, hiPSC-CMs generated by the SeV system show higher level of MLC-2a, TNNI-1, and TNT-2-adult gene expression than TNNI-3 and TNT-2-fetal gene expression. It is not clear from the results where the level of gene expression for MLC-2v falls. For the hiPSC-CMs derived from the episomal system, unfortunately the error bars are so large that concrete conclusions are difficult to draw both within the system and between the two reprogramming systems.

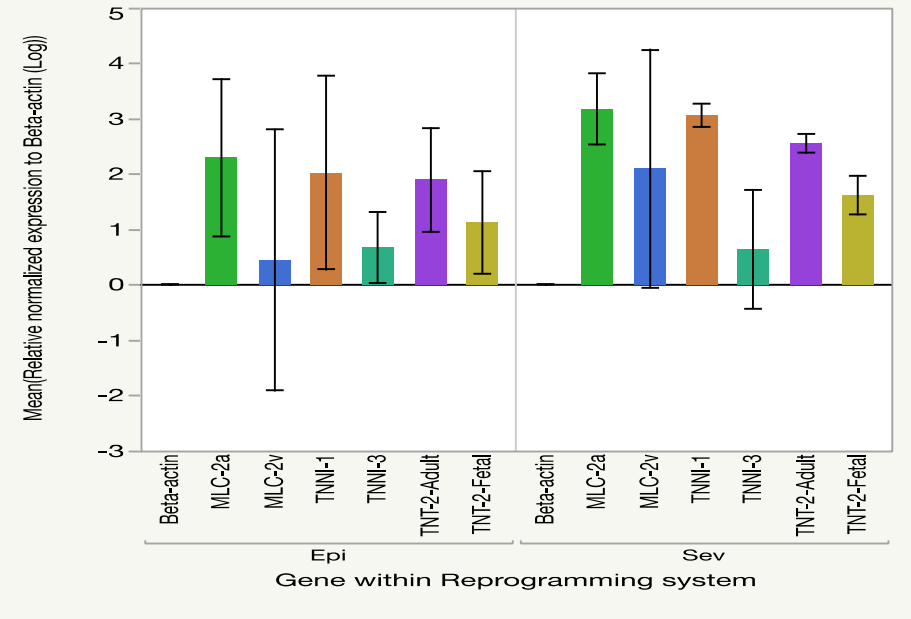

Figure 3.11 qRT-PCR analyses of cardiac specific markers in hiPSC-derived cardiomyocytes

CM cell lines were derived from hiPSCs generated using the episomal reprogramming system (n=6) two from donor Epii001, three from donor Epii003 and one from donor Epii004 and hiPSCs generated using the SeV system (n=3) two from donor SeVi001 and one from donor SeVi002. (Error bars shown as ± 1 SEM).

Table 3.3 Cardiac-specific markers in the SeV-derived and episomal-derived cardiomyocytes

	MLC-2a		MLC-2v		TNNI-1		TNNI-3		TNT-2-Fetal		TNT-2-Adult	
Reprogramming System	Mean	SE	Mean	SE	Mean	SE	Mean	SE	Mean	SE	Mean	SE
Sev	3.2	0.3	2.1	1.1	3.06	0.1	0.64	0.5	1.6	0.17	2.5	0.1
Epi	2.3	0.7	0.4	1.2	2.02	0.9	0.67	0.31	1.12	0.5	1.9	0.5

Although the CMs were examined for expression of cardiac specific markers on different days following differentiation (between days 39 and 66), no differences were observed in the expression of cardiac-specific genes in CMs derived from hiPSCs generated in either the SeV or episomal reprogramming systems.

Chapter 4. Discussion

4.1.1. T-cell activation: development of a successful protocol

Successful activation of T-cells prior to infection with Sev or transfection with episomal plasmids is a critical step in the reprogramming of donor-derived PBMCs. Results from the Trypan blue exclusion assays determined that, for the anti-CD3 plus IL-2 T-cell activation method, 10-20% of all cells died in days 1-2 following activation. However, a 20% increase in viability in days 3-5 occurred, followed by a stable population or decrease after days 5-6. Flow cytometry results confirmed the Trypan blue exclusion assay results, identifying the expanded population of viable cells as activated T-cells. 93-97% of the cells collected on day 5 post activation were positive for T-cell and activation markers. Phase contrast light microscopy provided a visual confirmation of the flow cytometry results, showing single cells at day 1 and aggregated cells, a characteristic of activated T-cells, at day 5 post activation. Together, these different experimental techniques show that the T-cell population from the donor's purified PBMCs has been successfully expanded and activated and that day 5 post activation is the optimal time for the reprogramming steps to be started. As well, the experiments were done using multiple samples, highlighting the fact that the activation and expansion protocols are replicable and can be standardized.

Flow cytometry was also used to determine which T-cell activation protocol, out of three, was the most effective in generating activated T-cells for use in the SeV reprogramming system. Compared to the 93% of cells testing positive for activation and T-cell markers, 5 days post activation, using the anti-CD3 plus IL-2 protocol, only 82% were positive using the Dynabeads plus IL-2 method in the same time frame. 6 days post activation, 75% of cells tested positive for activation and T-cell markers using the anti-CD3 plus IL-2 protocol but only 46% were positive using the anti-CD3 and anti-CD28 plus IL-2 procedure. These results showed that the most effective protocol for generating activated T-cells for SeV reprogramming is the anti-CD3 plus IL-2 method.

However, for both reprogramming systems, as indicated by the Trypan blue assay results, day 5 post activation is the time at which the maximum number of viable activated T-cells are present.

4.1.2. Identification and optimization of effective reprogramming methods

To assess the efficiency of different reprogramming methods in generating hiPSCs, one integrative method and two non-integrative methods (the SeV and episomal reprogramming systems) were tested. The integrative retro viral reprogramming method was attempted in three separate sets of experiments but was not successful in reprogramming PBMCs. All further experiments were then focused on the non-integrative methods.

One important step in successfully generating hiPSCs in the two non-integrative systems, the SeV and episomal systems, is optimizing the density of mitomycin-c inactivated MEF cells which act as a feeder layer for transfected PBMCs. After seeding MEF cells in densities between 3 and 7 x 10^5 cells/well on gelatin coated and non-coated 6-well plates for 9 days under transfection conditions without transfected cells, MEF cells on gelatin-coated plates with a density of 4 x 10^5 cells/well were found to best support the successful reprogramming and generation of hiPSCs in both reprogramming systems.

In addition to MEF cell density, nucleofection of episomal plasmids into the PBMCs was optimized as well by nucleofecting eGFP-episomal plasmids into both activated T-cells and unstimulated PBMCs. Flow cytometry analysis of eGFP expression revealed successful transfection of eGFP plasmids occurred in unstimulated PBMCs (with a transfection efficiency of 12 to 24%) but not in activated T-cells. This finding was supported by the experiment in which eGFP-episomal plasmids, transfected into activated T-cells using lipofectamine 3000, showed no eFGP expression over the course of one week post-transfection.

4.1.3. The relative success of the two reprogramming systems in generating hiPSCs

Having determined that the anti-CD3 antibodies plus IL-2 protocol is the most effective T-cell activation protocol for the SeV reprogramming system and that the maximum number of activated T-cells were present on day 5 post activation, the next step was to measure the success of transfection and transduction methods. Following the optimized version of Okita et al's episomal[63] reprogramming protocol (Dynabeads plus IL-2), and the optimized SeV method, both of which I developed, the efficiency of each method in generating hiPSCs was calculated. The SeV reprogramming system yielded 0.044% efficiency while the episomal system had 0.005% efficiency.

4.1.3.1 The generation and characterization of SeV- and episomally-derived hiPSCs

Twenty-one SeV derived hiPSC lines were generated from the activated T-cells of Donors 001 and 002 15-19 days after infection while 41 episomally-derived hiPSC lines were successfully generated from PBMCs of four donors in 21-24 days following transfection. The time for both methods, from blood drawing to generation of hiPSCs, was between 20-24 days.

Although the SeV system was nine times more efficient than the episomal system, phase contrast images showed that both systems produced hiPSCs with similar morphology, results confirmed by live cell staining which indicated the presence of the stem cell surface marker TRA-1-60. In terms of size and frequency, the hiPSC colonies from both systems were comparable, with the majority in the less than 100,000 μm^2 category (51% for the SeV and 59% for the episomal hiPSCs) and the 100,000 μm^2 to 200,000 μm^2 category (36% for both systems). More SeV system hiPSC colonies were larger than the episomal (3% of the SeV colonies had areas between 400,000 μm^2 and 500,000 μm^2 while no episomal colonies attained that large a size) and live cell staining for the differentiation marker CD44 revealed that a greater number of SeV hiPSC colonies were positive for this marker than episomal (20 out of 87 SeV colonies versus 4 out of 56 episomal colonies). Since differentiation occurs when colonies are overgrown, these findings are not unexpected.

The primary hiPSC colonies for both systems were generated after a similar length of time following transfection and transduction and were of equally good pluripotency. It was discovered that as the number of passages increased, the speed at which the hiPSCs grew to confluency also increased until stabilizing at approximately 3-4 days between passages. The hiPSCs generated from the two methods were then characterized for pluripotent surface markers and intracellular pluripotency gene expression at early passage (passage 5 or P5) and late passage (passage 10 or P10). Characterization for two pluripotent surface markers, SSEA-4 and TRA-1-60 using flow cytometry, revealed no differences between the reprogramming systems' hiPSCs and passage number. The standard error of the mean for SSEA-4 was close to the mean expression of this gene in both P5 and P10 while in contrast, TRA-1-60 produced a broader standard error of the mean in both. This suggests that SSEA-4 expression is a more accurate marker for the initial identification of hiPSCs.

Characterization for intracellular pluripotency gene expression using qRT-PCR at P5 and P10 showed that both SeV and episomally-derived hiPSCs expressed higher levels of Nanog and Oct4 and lower levels of c-Myc in both P5 and P10. No significant difference was observed between reprogramming systems and passage numbers based on expression of endogenous pluripotent markers.

In summary, the SeV reprogramming system was nine time more effective at generating hiPSCs from donor PBMCs than the episomal system. However, the hiPSCs generated from the SeV and episomal reprogramming systems were of equally good quality, as measured by visual morphology, speed of generation, size and numbers, presence of pluripotency surface markers (TRA-1-60 and SSEA-4), and endogenous pluripotent gene expression (Nanog, Oct4, and c-Myc). The pluripotency levels of the hiPSCs remained stable from early passage (P5) to late passage (P10).

4.1.3.2 The characterization of SeV- and episomally-derived hiPSC-CMs

With respect to assessing the functionality of P10 hiPSCs by their ability to differentiate into CMs, the results are inconclusive. While the qRT-PCR experiment to determine the levels of cardiac-specific gene expression in SeV and episomally-derived hiPSC-CMs showed higher levels of *MLC-2a*, *TNNI-1*, and *TNT-2* adult gene expression

than *TNNI-3* and *TNT-2*-fetal gene expression within the SeV system CMs, the error bars for the episomally derived CMs are so large that meaningful comparisons cannot be made, either within the episomal system or between the two systems.

Chapter 5. Future Directions and Conclusion

5.1. Future Directions

As with all research projects, the experimental results of this thesis generated many more questions to be addressed and experiments that can be done. Although there were no significant differences in the quality of the hiPSCs derived from the SeV and episomal reprogramming systems, high levels of variability in pluripotent gene expression were observed between the cell lines derived from each donor within each reprogramming system. Part of this problem, in the early passages (such as P5), is that, due to technique limitations, included among the hiPSCs are MEF cells and differentiated cells. The molecular footprints of these extraneous cells may be the source of some of the measured variability. In future to overcome this variability, cells could be sorted in early passages (such as P5) for the presence or absence of specific pluripotent markers. Based on the results of this thesis project, the variability of cell lines derived from each donor should be reduced prior to differentiation. Sorting pools of hiPSCs cell lines derived from each individual based on the presence or absence of the pluripotent surface marker, SSEA-4, which remained at the same level between early and late passages and reprogramming systems. This would provide a more homogenous, hiPSC lines from each donor. Then, differentiation protocols could be carried out on pools of hiPSCs from individual cell lines to determine which combinations of gene expression and protocol lead to successful differentiation[118], correlating different levels of pluripotent gene expression to different levels of cardiac specific marker expression.

The qRT-PCR experiment to measure the expression levels of cardiac-specific markers in hiPSC-derived CMs should be repeated. The error bars in the initial experiment prevented any meaningful conclusions from being made about the quality of hiSPC derived CMs in either the SeV or episomal systems. Future experiments to measure the expression of cardiac-specific markers on the first day hiPSC-derived CM cells begin beating, and at time points before and after this critical juncture, would aid in the early identification and tracking of these differentiated cells. Electrophysiological studies would complement these physiological functionality experiments.

Finally, because of the financial cost of these experiments, and stem cell research in general, the results of this research project are based on limited numbers (n = 3 to n = 6 with four blood donors in total). In future, replicating these experiments with larger sample numbers could decrease the variability and the standard error seen in these preliminary studies and allow more concrete conclusions to be made, particularly with respect to cardiac specific marker expression levels in hiPSC derived CMs.

5.2. Conclusion

The aims of this research project were to develop and optimize a standardized T-cell activation protocol for the SeV reprogramming system, optimize both the SeV and episomal reprogramming procedures for the generation of hiPSCs and determine which system was more effective, assess the pluripotency characteristics of the hiPSCs at both early and late passages, and examine their functionality as evidenced by their success at differentiating into cardiac cells. Although this thesis project did not definitively determine the functionality of P10 hiPSCs by their ability to differentiate into CMs, all other objectives were accomplished. A standardized T-cell activation protocol for the SeV reprogramming system was successfully created and both reprogramming procedures were optimized for the generation of hiPSCs. It was demonstrated that, although the SeV reprogramming system was nine times more efficient than the episomal system in generating hiPSCs, hiPSCs from both systems were similar, with respect to visual morphology, speed of generation, size and numbers, presence of pluripotency surface markers (TRA-1-60 and SSEA-4), and endogenous pluripotent gene expression (Nanog, Oct4, and c-Myc). The pluripotency levels of the hiPSCs from both systems were shown to remain stable from early passage to late. The findings generated by this thesis project are meaningful additions to the burgeoning field of hiPSC derived CM research and the development of human cardiovascular disease models.

References

1. Fuchs E, Segre JA. Stem cells: a new lease on life. Cell 2000;100(1):143-55.

2. De Los Angeles A, Ferrari F, Xi R, Fujiwara Y, Benvenisty N, Deng H, Hochedlinger K, Jaenisch R, Lee S, Leitch HG and others. Hallmarks of pluripotency. Nature 2015;525(7570):469-78.

3. Kelly SJ. Studies of the developmental potential of 4- and 8-cell stage mouse blastomeres. J Exp Zool 1977;200(3):365-76.

4. Rideout WM, 3rd, Eggan K, Jaenisch R. Nuclear cloning and epigenetic reprogramming of the genome. Science 2001;293(5532):1093-8.

5. Tarkowski AK. Experiments on the development of isolated blastomers of mouse eggs. Nature 1959;184:1286-7.

6. Bradley A, Evans M, Kaufman MH, Robertson E. Formation of germ-line chimaeras from embryo-derived teratocarcinoma cell lines. Nature 1984;309(5965):255-6.

7. Ratajczak MZ, Zuba-Surma EK, Wysoczynski M, Wan W, Ratajczak J, Wojakowski W, Kucia M. Hunt for pluripotent stem cell -- regenerative medicine search for almighty cell. J Autoimmun 2008;30(3):151-62.

8. Colter DC, Sekiya I, Prockop DJ. Identification of a subpopulation of rapidly self-renewing and multipotential adult stem cells in colonies of human marrow stromal cells. Proc Natl Acad Sci U S A 2001;98(14):7841-5.

9. Choi HW, Kim JS, Hong YJ, Song H, Seo HG, Do JT. In vivo reprogrammed pluripotent stem cells from teratomas share analogous properties with their in vitro counterparts. Sci Rep 2015;5:13559.

10. Zhao T, Zhang ZN, Rong Z, Xu Y. Immunogenicity of induced pluripotent stem cells. Nature 2011;474(7350):212-5.

11. Giorgetti A, Montserrat N, Aasen T, Gonzalez F, Rodriguez-Piza I, Vassena R, Raya A, Boue S, Barrero MJ, Corbella BA and others. Generation of induced pluripotent stem cells from human cord blood using OCT4 and SOX2. Cell Stem Cell 2009;5(4):353-7.

12. Aasen T, Raya A, Barrero MJ, Garreta E, Consiglio A, Gonzalez F, Vassena R, Bilic J, Pekarik V, Tiscornia G and others. Efficient and rapid generation of induced pluripotent stem cells from human keratinocytes. Nat Biotechnol 2008;26(11):1276-84.

13. Loh YH, Agarwal S, Park IH, Urbach A, Huo H, Heffner GC, Kim K, Miller JD, Ng K, Daley GQ. Generation of induced pluripotent stem cells from human blood. Blood 2009;113(22):5476-9.

14. Strachan T, Lindsay S, Wilson DI. Molecular genetics of early human development. Oxford ; Herndon, VA: BIOS Scientific Publishers; 1997. xiv, 265 p. p.

15. Hamlin RL, Altschuld RA. Extrapolation from mouse to man. Circ Cardiovasc Imaging 2011;4(1):2-4.

16. Saenger P. Turner's syndrome. N Engl J Med 1996;335(23):1749-54.

17. Avior Y, Sagi I, Benvenisty N. Pluripotent stem cells in disease modelling and drug discovery. Nat Rev Mol Cell Biol 2016;17(3):170-82.

18. Urbach A, Schuldiner M, Benvenisty N. Modeling for Lesch-Nyhan disease by gene targeting in human embryonic stem cells. Stem Cells 2004;22(4):635-41.

19. Wang S, Bates J, Li X, Schanz S, Chandler-Militello D, Levine C, Maherali N, Studer L, Hochedlinger K, Windrem M and others. Human iPSC-derived oligodendrocyte progenitor cells can myelinate and rescue a mouse model of congenital hypomyelination. Cell Stem Cell 2013;12(2):252-64.

20. Mariani J, Simonini MV, Palejev D, Tomasini L, Coppola G, Szekely AM, Horvath TL, Vaccarino FM. Modeling human cortical development in vitro using induced pluripotent stem cells. Proc Natl Acad Sci U S A 2012;109(31):12770-5.

21. Roessler R, Smallwood SA, Veenvliet JV, Pechlivanoglou P, Peng SP, Chakrabarty K, Groot-Koerkamp MJ, Pasterkamp RJ, Wesseling E, Kelsey G and others. Detailed analysis of the genetic and epigenetic signatures of iPSC-derived mesodiencephalic dopaminergic neurons. Stem Cell Reports 2014;2(4):520-33.

22. Chester N, Kuo F, Kozak C, O'Hara CD, Leder P. Stage-specific apoptosis, developmental delay, and embryonic lethality in mice homozygous for a targeted disruption in the murine Bloom's syndrome gene. Genes Dev 1998;12(21):3382-93.

23. Morris JK, Wald NJ, Watt HC. Fetal loss in Down syndrome pregnancies. Prenat Diagn 1999;19(2):142-5.

24. Collins FS, Varmus H. A new initiative on precision medicine. N Engl J Med 2015;372(9):793-5.

25. Chen IY, Matsa E, Wu JC. Induced pluripotent stem cells: at the heart of cardiovascular precision medicine. Nat Rev Cardiol 2016.

26. Sallam K, Li Y, Sager PT, Houser SR, Wu JC. Finding the rhythm of sudden cardiac death: new opportunities using induced pluripotent stem cell-derived cardiomyocytes. Circ Res 2015;116(12):1989-2004.

27. Frommeyer G, Eckardt L. Drug-induced proarrhythmia: risk factors and electrophysiological mechanisms. Nat Rev Cardiol 2016;13(1):36-47.

28. King TJ, Briggs R. Changes in the Nuclei of Differentiating Gastrula Cells, as Demonstrated by Nuclear Transplantation. Proc Natl Acad Sci U S A 1955;41(5):321-5.

29. Gurdon JB. The developmental capacity of nuclei taken from intestinal epithelium cells of feeding tadpoles. J Embryol Exp Morphol 1962;10:622-40.

30. Gurdon JB, Laskey RA, Reeves OR. The developmental capacity of nuclei transplanted from keratinized skin cells of adult frogs. J Embryol Exp Morphol 1975;34(1):93-112.

31. Tokuzawa Y, Kaiho E, Maruyama M, Takahashi K, Mitsui K, Maeda M, Niwa H, Yamanaka S. Fbx15 is a novel target of Oct3/4 but is dispensable for embryonic stem cell self-renewal and mouse development. Mol Cell Biol 2003;23(8):2699-708.

32. Takahashi K, Yamanaka S. Induction of pluripotent stem cells from mouse embryonic and adult fibroblast cultures by defined factors. Cell 2006;126(4):663-76.

33. Seki T, Yuasa S, Fukuda K. Generation of induced pluripotent stem cells from a small amount of human peripheral blood using a combination of activated T cells and Sendai virus. Nat Protoc 2012;7(4):718-28.

34. Seki T, Yuasa S, Oda M, Egashira T, Yae K, Kusumoto D, Nakata H, Tohyama S, Hashimoto H, Kodaira M and others. Generation of induced pluripotent stem cells from human terminally differentiated circulating T cells. Cell Stem Cell 2010;7(1):11-4.

35. Pereira L, Yi F, Merrill BJ. Repression of Nanog gene transcription by Tcf3 limits embryonic stem cell self-renewal. Mol Cell Biol 2006;26(20):7479-91.

36. Takahashi K, Tanabe K, Ohnuki M, Narita M, Ichisaka T, Tomoda K, Yamanaka S. Induction of pluripotent stem cells from adult human fibroblasts by defined factors. Cell 2007;131(5):861-72.

37. Li W, Wei W, Zhu S, Zhu J, Shi Y, Lin T, Hao E, Hayek A, Deng H, Ding S. Generation of rat and human induced pluripotent stem cells by combining genetic reprogramming and chemical inhibitors. Cell Stem Cell 2009;4(1):16-9.

38. Liu H, Zhu F, Yong J, Zhang P, Hou P, Li H, Jiang W, Cai J, Liu M, Cui K and others. Generation of induced pluripotent stem cells from adult rhesus monkey fibroblasts. Cell Stem Cell 2008;3(6):587-90.

39. Loh YH, Wu Q, Chew JL, Vega VB, Zhang W, Chen X, Bourque G, George J, Leong B, Liu J and others. The Oct4 and Nanog transcription network regulates pluripotency in mouse embryonic stem cells. Nat Genet 2006;38(4):431-40.

40. Boyer LA, Lee TI, Cole MF, Johnstone SE, Levine SS, Zucker JP, Guenther MG, Kumar RM, Murray HL, Jenner RG and others. Core transcriptional regulatory circuitry in human embryonic stem cells. Cell 2005;122(6):947-56.

41. Chambers I, Colby D, Robertson M, Nichols J, Lee S, Tweedie S, Smith A. Functional expression cloning of Nanog, a pluripotency sustaining factor in embryonic stem cells. Cell 2003;113(5):643-55.

42. Nichols J, Zevnik B, Anastassiadis K, Niwa H, Klewe-Nebenius D, Chambers I, Scholer H, Smith A. Formation of pluripotent stem cells in the mammalian embryo depends on the POU transcription factor Oct4. Cell 1998;95(3):379-91.

43. Mitsui K, Tokuzawa Y, Itoh H, Segawa K, Murakami M, Takahashi K, Maruyama M, Maeda M, Yamanaka S. The homeoprotein Nanog is required for maintenance of pluripotency in mouse epiblast and ES cells. Cell 2003;113(5):631-42.

44. Reubinoff BE, Pera MF, Fong CY, Trounson A, Bongso A. Embryonic stem cell lines from human blastocysts: somatic differentiation in vitro. Nat Biotechnol 2000;18(4):399-404.

45. Spar D. The egg trade--making sense of the market for human oocytes. N Engl J Med 2007;356(13):1289-91.

46. Guan X, Mack DL, Moreno CM, Strande JL, Mathieu J, Shi Y, Markert CD, Wang Z, Liu G, Lawlor MW and others. Dystrophin-deficient cardiomyocytes derived from human urine: new biologic reagents for drug discovery. Stem Cell Res 2014;12(2):467-80.

47. Raab S, Klingenstein M, Liebau S, Linta L. A Comparative View on Human Somatic Cell Sources for iPSC Generation. Stem Cells Int 2014;2014:768391.

48. Takahashi K, Okita K, Nakagawa M, Yamanaka S. Induction of pluripotent stem cells from fibroblast cultures. Nat Protoc 2007;2(12):3081-9.

49. Okita K, Ichisaka T, Yamanaka S. Generation of germline-competent induced pluripotent stem cells. Nature 2007;448(7151):313-U1.

50. Fusaki N, Ban H, Nishiyama A, Saeki K, Hasegawa M. Efficient induction of transgene-free human pluripotent stem cells using a vector based on Sendai virus, an RNA virus that does not integrate into the host genome. Proc Jpn Acad Ser B Phys Biol Sci 2009;85(8):348-62.

51. Yusa K, Rad R, Takeda J, Bradley A. Generation of transgene-free induced pluripotent mouse stem cells by the piggyBac transposon. Nat Methods 2009;6(5):363-9.

52. Warren L, Manos PD, Ahfeldt T, Loh YH, Li H, Lau F, Ebina W, Mandal PK, Smith ZD, Meissner A and others. Highly efficient reprogramming to pluripotency and directed differentiation of human cells with synthetic modified mRNA. Cell Stem Cell 2010;7(5):618-30.

53. Yu J, Hu K, Smuga-Otto K, Tian S, Stewart R, Slukvin, II, Thomson JA. Human induced pluripotent stem cells free of vector and transgene sequences. Science 2009;324(5928):797-801.

54. Ban H, Nishishita N, Fusaki N, Tabata T, Saeki K, Shikamura M, Takada N, Inoue M, Hasegawa M, Kawamata S and others. Efficient generation of transgene-free human induced pluripotent stem cells (iPSCs) by temperature-sensitive Sendai virus vectors. Proc Natl Acad Sci U S A 2011;108(34):14234-9.

55. Stadtfeld M, Nagaya M, Utikal J, Weir G, Hochedlinger K. Induced pluripotent stem cells generated without viral integration. Science 2008;322(5903):945-9.

56. Gonzalez F, Barragan Monasterio M, Tiscornia G, Montserrat Pulido N, Vassena R, Batlle Morera L, Rodriguez Piza I, Izpisua Belmonte JC. Generation of mouse-induced pluripotent stem cells by transient expression of a single nonviral polycistronic vector. Proc Natl Acad Sci U S A 2009;106(22):8918-22.

57. MacArthur BD, Sevilla A, Lenz M, Muller FJ, Schuldt BM, Schuppert AA, Ridden SJ, Stumpf PS, Fidalgo M, Ma'ayan A and others. Nanog-dependent feedback loops regulate murine embryonic stem cell heterogeneity. Nat Cell Biol 2012;14(11):1139-47.

58. Lamb RA KD. Paramyxoviridae: The viruses and their replication. In: Fields BN, Knipe DM, Howley PM, editors. Fields Virology. 3rd ed. New York: Raven Press; 1996. p 2 v. (xxi, 2950, 97 p.).

59. Li HO, Zhu YF, Asakawa M, Kuma H, Hirata T, Ueda Y, Lee YS, Fukumura M, Iida A, Kato A and others. A cytoplasmic RNA vector derived from nontransmissible Sendai virus with efficient gene transfer and expression. J Virol 2000;74(14):6564-9.

60. Nagai Y TA, Irie T, Yonemitsu M, Gotoh B. The journey from mouse pathogen to a state-of-the-art tool in virus research and biotechnology. In: Samal SK, editor. The biology of paramyxoviruses. Norfolk, UK: Caister Academic Press; 2011. p vii, 469 p.

61. Pollack Y, Stein R, Razin A, Cedar H. Methylation of foreign DNA sequences in eukaryotic cells. Proc Natl Acad Sci U S A 1980;77(11):6463-7.

62. Okita K, Matsumura Y, Sato Y, Okada A, Morizane A, Okamoto S, Hong H, Nakagawa M, Tanabe K, Tezuka K and others. A more efficient method to generate integration-free human iPS cells. Nat Methods 2011;8(5):409-12.

63. Okita K, Yamakawa T, Matsumura Y, Sato Y, Amano N, Watanabe A, Goshima N, Yamanaka S. An efficient nonviral method to generate integration-free human-induced pluripotent stem cells from cord blood and peripheral blood cells. Stem Cells 2013;31(3):458-66.

64. Heng JC, Feng B, Han J, Jiang J, Kraus P, Ng JH, Orlov YL, Huss M, Yang L, Lufkin T and others. The nuclear receptor Nr5a2 can replace Oct4 in the reprogramming of murine somatic cells to pluripotent cells. Cell Stem Cell 2010;6(2):167-74.

65. Han J, Yuan P, Yang H, Zhang J, Soh BS, Li P, Lim SL, Cao S, Tay J, Orlov YL and others. Tbx3 improves the germ-line competency of induced pluripotent stem cells. Nature 2010;463(7284):1096-100.

66. Buganim Y, Faddah DA, Cheng AW, Itskovich E, Markoulaki S, Ganz K, Klemm SL, van Oudenaarden A, Jaenisch R. Single-cell expression analyses during cellular reprogramming reveal an early stochastic and a late hierarchic phase. Cell 2012;150(6):1209-22.

67. Schmidt R, Plath K. The roles of the reprogramming factors Oct4, Sox2 and Klf4 in resetting the somatic cell epigenome during induced pluripotent stem cell generation. Genome Biol 2012;13(10):251.

68. Koche RP, Smith ZD, Adli M, Gu H, Ku M, Gnirke A, Bernstein BE, Meissner A. Reprogramming factor expression initiates widespread targeted chromatin remodeling. Cell Stem Cell 2011;8(1):96-105.

69. Maherali N, Sridharan R, Xie W, Utikal J, Eminli S, Arnold K, Stadtfeld M, Yachechko R, Tchieu J, Jaenisch R and others. Directly reprogrammed fibroblasts show global epigenetic remodeling and widespread tissue contribution. Cell Stem Cell 2007;1(1):55-70.

70. Fussner E, Djuric U, Strauss M, Hotta A, Perez-Iratxeta C, Lanner F, Dilworth FJ, Ellis J, Bazett-Jones DP. Constitutive heterochromatin reorganization during somatic cell reprogramming. EMBO J 2011;30(9):1778-89.

71. Siedner S, Kruger M, Schroeter M, Metzler D, Roell W, Fleischmann BK, Hescheler J, Pfitzer G, Stehle R. Developmental changes in contractility and sarcomeric proteins from the early embryonic to the adult stage in the mouse heart. J Physiol 2003;548(Pt 2):493-505.

72. Samavarchi-Tehrani P, Golipour A, David L, Sung HK, Beyer TA, Datti A, Woltjen K, Nagy A, Wrana JL. Functional genomics reveals a BMP-driven mesenchymal-to-epithelial transition in the initiation of somatic cell reprogramming. Cell Stem Cell 2010;7(1):64-77.

73. Li R, Liang J, Ni S, Zhou T, Qing X, Li H, He W, Chen J, Li F, Zhuang Q and others. A mesenchymal-to-epithelial transition initiates and is required for the nuclear reprogramming of mouse fibroblasts. Cell Stem Cell 2010;7(1):51-63.

74. Polo JM, Anderssen E, Walsh RM, Schwarz BA, Nefzger CM, Lim SM, Borkent M, Apostolou E, Alaei S, Cloutier J and others. A molecular roadmap of reprogramming somatic cells into iPS cells. Cell 2012;151(7):1617-32.

75. Wakayama S, Jakt ML, Suzuki M, Araki R, Hikichi T, Kishigami S, Ohta H, Van Thuan N, Mizutani E, Sakaide Y and others. Equivalency of nuclear transfer-derived embryonic stem cells to those derived from fertilized mouse blastocysts. Stem Cells 2006;24(9):2023-33.

76. Brambrink T, Hochedlinger K, Bell G, Jaenisch R. ES cells derived from cloned and fertilized blastocysts are transcriptionally and functionally indistinguishable. Proc Natl Acad Sci U S A 2006;103(4):933-8.

77. Golipour A, David L, Liu Y, Jayakumaran G, Hirsch CL, Trcka D, Wrana JL. A late transition in somatic cell reprogramming requires regulators distinct from the pluripotency network. Cell Stem Cell 2012;11(6):769-82.

78. Hansson J, Rafiee MR, Reiland S, Polo JM, Gehring J, Okawa S, Huber W, Hochedlinger K, Krijgsveld J. Highly coordinated proteome dynamics during reprogramming of somatic cells to pluripotency. Cell Rep 2012;2(6):1579-92.

79. Costello E, Munoz M, Buetti E, Meylan PR, Diggelmann H, Thali M. Gene transfer into stimulated and unstimulated T lymphocytes by HIV-1-derived lentiviral vectors. Gene Ther 2000;7(7):596-604.

80. Chen L, Flies DB. Molecular mechanisms of T cell co-stimulation and co-inhibition. Nat Rev Immunol 2013;13(4):227-42.

81. Toribio ML, De la Hera A, Marcos MA, Marquez C, Martinez C. Activation of the interleukin 2 pathway precedes CD3-T cell receptor expression in thymic development. Differential growth requirements of early and mature intrathymic subpopulations. Eur J Immunol 1989;19(1):9-15.

82. Tsoukas CD, Landgraf B, Bentin J, Valentine M, Lotz M, Vaughan JH, Carson DA. Activation of resting T lymphocytes by anti-CD3 (T3) antibodies in the absence of monocytes. J Immunol 1985;135(3):1719-23.

83. Iezzi G, Karjalainen K, Lanzavecchia A. The duration of antigenic stimulation determines the fate of naive and effector T cells. Immunity 1998;8(1):89-95.

84. Hedfors IA, Brinchmann JE. Long-term proliferation and survival of in vitro-activated T cells is dependent on Interleukin-2 receptor signalling but not on the high-affinity IL-2R. Scand J Immunol 2003;58(5):522-32.

85. Zappasodi R, Di Nicola M, Carlo-Stella C, Mortarini R, Molla A, Vegetti C, Albani S, Anichini A, Gianni AM. The effect of artificial antigen-presenting cells with preclustered anti-CD28/-CD3/-LFA-1 monoclonal antibodies on the induction of ex vivo expansion of functional human antitumor T cells. Haematologica 2008;93(10):1523-34.

86. June CH, Ledbetter JA, Gillespie MM, Lindsten T, Thompson CB. T-cell proliferation involving the CD28 pathway is associated with cyclosporine-resistant interleukin 2 gene expression. Mol Cell Biol 1987;7(12):4472-81.

87. MacArthur BD, Lemischka IR. Statistical mechanics of pluripotency. Cell 2013;154(3):484-9.

88. Marti M, Mulero L, Pardo C, Morera C, Carrio M, Laricchia-Robbio L, Esteban CR, Izpisua Belmonte JC. Characterization of pluripotent stem cells. Nat Protoc 2013;8(2):223-53.

89. Canham MA, Sharov AA, Ko MS, Brickman JM. Functional heterogeneity of embryonic stem cells revealed through translational amplification of an early endodermal transcript. PLoS Biol 2010;8(5):e1000379.

90. Chambers I, Silva J, Colby D, Nichols J, Nijmeijer B, Robertson M, Vrana J, Jones K, Grotewold L, Smith A. Nanog safeguards pluripotency and mediates germline development. Nature 2007;450(7173):1230-4.

91. Hayashi K, Lopes SM, Tang F, Surani MA. Dynamic equilibrium and heterogeneity of mouse pluripotent stem cells with distinct functional and epigenetic states. Cell Stem Cell 2008;3(4):391-401.

92. Kobayashi T, Mizuno H, Imayoshi I, Furusawa C, Shirahige K, Kageyama R. The cyclic gene Hes1 contributes to diverse differentiation responses of embryonic stem cells. Genes Dev 2009;23(16):1870-5.

93. Marvin MJ, Di Rocco G, Gardiner A, Bush SM, Lassar AB. Inhibition of Wnt activity induces heart formation from posterior mesoderm. Genes Dev 2001;15(3):316-27.

94. Olson EN. Development. The path to the heart and the road not taken. Science 2001;291(5512):2327-8.

95. Schneider VA, Mercola M. Wnt antagonism initiates cardiogenesis in Xenopus laevis. Genes Dev 2001;15(3):304-15.

96. Pashmforoush M, Lu JT, Chen H, Amand TS, Kondo R, Pradervand S, Evans SM, Clark B, Feramisco JR, Giles W and others. Nkx2-5 pathways and congenital heart disease; loss of ventricular myocyte lineage specification leads to progressive cardiomyopathy and complete heart block. Cell 2004;117(3):373-86.

97. Ishiwata T, Nakazawa M, Pu WT, Tevosian SG, Izumo S. Developmental changes in ventricular diastolic function correlate with changes in ventricular myoarchitecture in normal mouse embryos. Circ Res 2003;93(9):857-65.

98. Zhou B, Ma Q, Rajagopal S, Wu SM, Domian I, Rivera-Feliciano J, Jiang D, von Gise A, Ikeda S, Chien KR and others. Epicardial progenitors contribute to the cardiomyocyte lineage in the developing heart. Nature 2008;454(7200):109-13.

99. Christoffels VM, Grieskamp T, Norden J, Mommersteeg MT, Rudat C, Kispert A. Tbx18 and the fate of epicardial progenitors. Nature 2009;458(7240):E8-9; discussion E9-10.

100. Li MX, Robertson IM, Sykes BD. Interaction of cardiac troponin with cardiotonic drugs: a structural perspective. Biochem Biophys Res Commun 2008;369(1):88-99.

101. Bhavsar PK, Brand NJ, Yacoub MH, Barton PJ. Isolation and characterization of the human cardiac troponin I gene (TNNI3). Genomics 1996;35(1):11-23.

102. Wade R, Eddy R, Shows TB, Kedes L. cDNA sequence, tissue-specific expression, and chromosomal mapping of the human slow-twitch skeletal muscle isoform of troponin I. Genomics 1990;7(3):346-57.

103. Tiso N, Rampoldi L, Pallavicini A, Zimbello R, Pandolfo D, Valle G, Lanfranchi G, Danieli GA. Fine mapping of five human skeletal muscle genes: alpha-tropomyosin, beta-tropomyosin, troponin-I slow-twitch, troponin-I fast-twitch, and troponin-C fast. Biochem Biophys Res Commun 1997;230(2):347-50.

104. Bhavsar PK, Dhoot GK, Cumming DV, Butler-Browne GS, Yacoub MH, Barton PJ. Developmental expression of troponin I isoforms in fetal human heart. FEBS Lett 1991;292(1-2):5-8.

105. Hunkeler NM, Kullman J, Murphy AM. Troponin I isoform expression in human heart. Circ Res 1991;69(5):1409-14.

106. Sasse S, Brand NJ, Kyprianou P, Dhoot GK, Wade R, Arai M, Periasamy M, Yacoub MH, Barton PJ. Troponin I gene expression during human cardiac development and in end-stage heart failure. Circ Res 1993;72(5):932-8.

107. Bhavsar PK, Dellow KA, Yacoub MH, Brand NJ, Barton PJ. Identification of cis-acting DNA elements required for expression of the human cardiac troponin I gene promoter. J Mol Cell Cardiol 2000;32(1):95-108.

108. Dellow KA, Bhavsar PK, Brand NJ, Barton PJ. Identification of novel, cardiac-restricted transcription factors binding to a CACC-box within the human cardiac troponin I promoter. Cardiovasc Res 2001;50(1):24-33.

109. Bodor GS, Porterfield D, Voss EM, Smith S, Apple FS. Cardiac troponin-I is not expressed in fetal and healthy or diseased adult human skeletal muscle tissue. Clin Chem 1995;41(12 Pt 1):1710-5.

110. Mesnard L, Logeart D, Taviaux S, Diriong S, Mercadier JJ, Samson F. Human cardiac troponin T: cloning and expression of new isoforms in the normal and failing heart. Circ Res 1995;76(4):687-92.

111. Townsend PJ, Farza H, MacGeoch C, Spurr NK, Wade R, Gahlmann R, Yacoub MH, Barton PJ. Human cardiac troponin T: identification of fetal isoforms and assignment of the TNNT2 locus to chromosome 1q. Genomics 1994;21(2):311-6.

112. Barton PJ, Felkin LE, Koban MU, Cullen ME, Brand NJ, Dhoot GK. The slow skeletal muscle troponin T gene is expressed in developing and diseased human heart. Mol Cell Biochem 2004;263(1-2):91-7.

113. Anderson PA, Oakeley AE. Immunological identification of five troponin T isoforms reveals an elaborate maturational troponin T profile in rabbit myocardium. Circ Res 1989;65(4):1087-93.

114. Samson F, Mesnard L, Mihovilovic M, Potter TG, Mercadier JJ, Roses AD, Gilbert JR. A new human slow skeletal troponin T (TnTs) mRNA isoform derived from alternative splicing of a single gene. Biochem Biophys Res Commun 1994;199(2):841-7.

115. Jin JP, Chen A, Huang QQ. Three alternatively spliced mouse slow skeletal muscle troponin T isoforms: conserved primary structure and regulated expression during postnatal development. Gene 1998;214(1-2):121-9.

116. Lian X, Zhang J, Azarin SM, Zhu K, Hazeltine LB, Bao X, Hsiao C, Kamp TJ, Palecek SP. Directed cardiomyocyte differentiation from human pluripotent stem cells by modulating Wnt/beta-catenin signaling under fully defined conditions. Nat Protoc 2013;8(1):162-75.

117. Human Induced Pluripotent Stem Cell (iPSC) Handling Protocols (MEF Feeder Layer). In: Research CIFM, editor.

118. Rajala K, Pekkanen-Mattila M, Aalto-Setala K. Cardiac differentiation of pluripotent stem cells. Stem Cells Int 2011;2011:383709.

Appendix A.

Consent Form

SFU molecularcardiac PHYSIOLOGY GROUP

Title of Study: Isolation and activation of T cells from human blood

Principal Investigator: Glen F Tibbits, PhD
Professor and Chair
Canada Research Chair in Molecular Cardiac Physiology
Dept. of Biomedical Physiology and Kinesiology
Simon Fraser University
Tel: [redacted]
E-mail: [redacted]

Sponsors: Canadian Institutes of Health Research
Natural Sciences and Engineering Research Council
Simon Fraser University

Emergency Telephone Number: [redacted]

You are being invited to take part in this research study because you are in good health, not pregnant, and have never been diagnosed with hepatitis B or C, HIV infection, or any other transmissible infectious disease.

Your participation is entirely voluntary, so it is up to you to decide whether or not to take part in this study. Before you decide, it is important for you to understand why the research is being done and what it will involve. If you wish to participate, you will be asked to sign this form. You do not have to provide any reason should you decide not to participate. Should you refuse to participate or withdraw, it would not in any way jeopardize your future medical care.

This study is being conducted by Dr. Glen Tibbits at Simon Fraser University. Our research is sponsored by the Canadian Institutes of Health Research and the Natural Sciences and Engineering Research Council of Canada.

The purpose of this study is to develop new ways to improve the diagnosis and treatment of inherited cardiac arrhythmias and cardiomyopathies. The T cells that we will isolate from your blood sample will be used to make inducible pluripotent stem cells (iPSCs) which in turn will be used to make beating heart cells (cardiomyocytes) that carry your genetic information. We will then test the properties of the cardiomyocytes for comparison with those who harbor genetic mutations that underlie (or put them at risk for) serious cardiac diseases.

This study requires blood from healthy subjects, and could not be conveniently performed with any alternate source of biological material.

If you agree to take part in this study, the procedures you can expect will include the following:

- A brief physical exam to measure blood pressure and a finger prick to test for anemia
- Blood withdrawal from a vein in your arm through a sterile needle by a trained phlembotomist. You may experience momentary discomfort associated with insertion of the needle, and a small bruise occasionally occurs at the puncture site.
- 50 mL of blood will be collected (equal to about 1/10 of a standard donation at Canadian Blood Services)
- Although the amount of blood to be removed will be less than 1% of your total blood volume, you may experience lightheadedness or dizziness. This is usually a reaction to discomfort from the needle. If this occurs during the blood withdrawal, the procedure will be stopped. The dizziness subsides after a few minutes of rest.

The procedure will take approximately 10 minutes, and you will be asked to stay seated for an additional 10-15 minutes to ensure you have recovered from any lightheadedness or dizziness. The blood that was removed will be regenerated by the bone marrow in less than one week, and there are no long-term side effects associated with the procedure. The maximum amount of blood that can be donated is 100 mL every month.

The cells from your blood may be employed immediately and will be used strictly for research in the current study. No other investigators will have access to the material, and it will not be stored as part of the inventory of a blood bank.

Your confidentiality will be respected. No information that discloses your identity will be released or published. Your identity will be recorded in a confidential logbook; however, no records which identify you by name or initials will be allowed to leave the Investigators' office. However, you should be aware that your blood may be tested for the presence of infection with Hepatitis C and/or HIV-1 and -2. Pre-testing counseling will be made available upon request. Should any one of these tests give a positive result, we are obligated by law to report these results to the BC Centre for Disease Control, and they will become part of your permanent health record.

The investigators and/or their partners/immediate family members will not receive any personal benefits connected to this research study.

You should understand that Canadian legislation prohibits the sale of human tissues, including blood. You will however receive light refreshments following donation.

Any complaints or concerns can be address to Dr. Hal Weinberg, Director, The Office of Research Ethics at [redacted] or [redacted] If you have any questions or desire further information about this study before, during or after participation, you can contact Dr. Glen Tibbits anytime, 7 days a week, at [redacted] You may also contact Dr. Tibbits should you wish to be informed of the progress in this project, and/or of the results of the research.

Appendix B.

Protocols

Human Cell Isolation (SEPMATE PROCEDURE)

(http://www.stemcell.com/~/media/TechnicalResources/6/D/4/9/D/29251PIS.pdf?la=en)

Mitomycin C Treatment of Mouse embryonic Fibroblast cells

(http://www.amsbio.com/brochures/Mitomycin_C_Treatment_of_Fibroblasts.pdf)

Transfection with episomal plasmid

(http://www.cira.kyoto-u.ac.jp/e/research/img/protocol/Tcell-iPS_Protocol.pdf)

Infection with Sendai virus

http://www.nature.com/nprot/journal/v7/n4/pdf/nprot.2012.015.pdf

Preparing matrigel coated plates

(http://www.wicell.org/media.acux/39c0a534-577e-4850-aede-d91e1322e479)

Cryopreservation of hiPSCs

(http://www.amsbio.com/datasheets/11897.pdf)

Immunocytochemistry of Live cells

(https://tools.thermofisher.com/content/sfs/manuals/stemcell_ab_kits_live_cell_imaging_man.pdf)

Pluripotent Surface marker staining

- **PE Mouse anti-SSEA-4**

https://tools.thermofisher.com/content/sfs/manuals/stemcell_ab_kits_live_cell_imaging_man.pdf

- **Alexa Fluor 647 Mouse anti-Human TRA-1-60 Antigen**

http://www.bdbiosciences.com/ds/pm/tds/560850.pdf

RNA extraction

- **Qiagen RNeasy Mini Kit**

https://www.qiagen.com/us/resources/resourcedetail?id=0e32fbb1-c307-4603-ac81-a5e98490ed23&lang=en

Reverse transcription

QuantiTect Reverse Transcription Kit

(https://www.qiagen.com/us/resources/resourcedetail?id=a7889bfb-cb1b-4e23-a538-9e4f20fdca91&lang=en)

Primer Sequences for pluripotent genes

Primers of pluripotent genes	Sequence (5’ → 3’)
Sox2 FWD	TTA AGG ATC CCA GTG TGG TGG T
Sox2 REV	GCT TCA GCT CCG TCT CCA TCA
cMyc FWD	TAC TGC GAC GAG GAG GAG AA
cMyc REV	CGA AGG GAG AAG GGT GTG AC
Klf4 FWD	AGT GTG GTG GTA CGG GAA ATC
Klf4 REV	CGT GGA GAA AGA TGG GAG CA
Oct 4 FWD	GTG GAG GAA GCT GAC AAC AA
Oct 4 REV	ATT CTC CAG GTT GCC TCT CA
Nanog FWD	AAG AGG TGG CAG AAA AAC AAC T
Nanog REV	CTG GAT GTT CTG GGT CTG GT
ZFP-42 FWD	GCAACTGAAGAAACGGGCAA
ZFP-42 REV	AACTCACCCCTTATGACGCA
B-Actin FWD	ATT GCC GAC AGG ATG CAG AA
B-Actin REV	GGG CCG GAC TCG TCA TAC TC

Appendix C

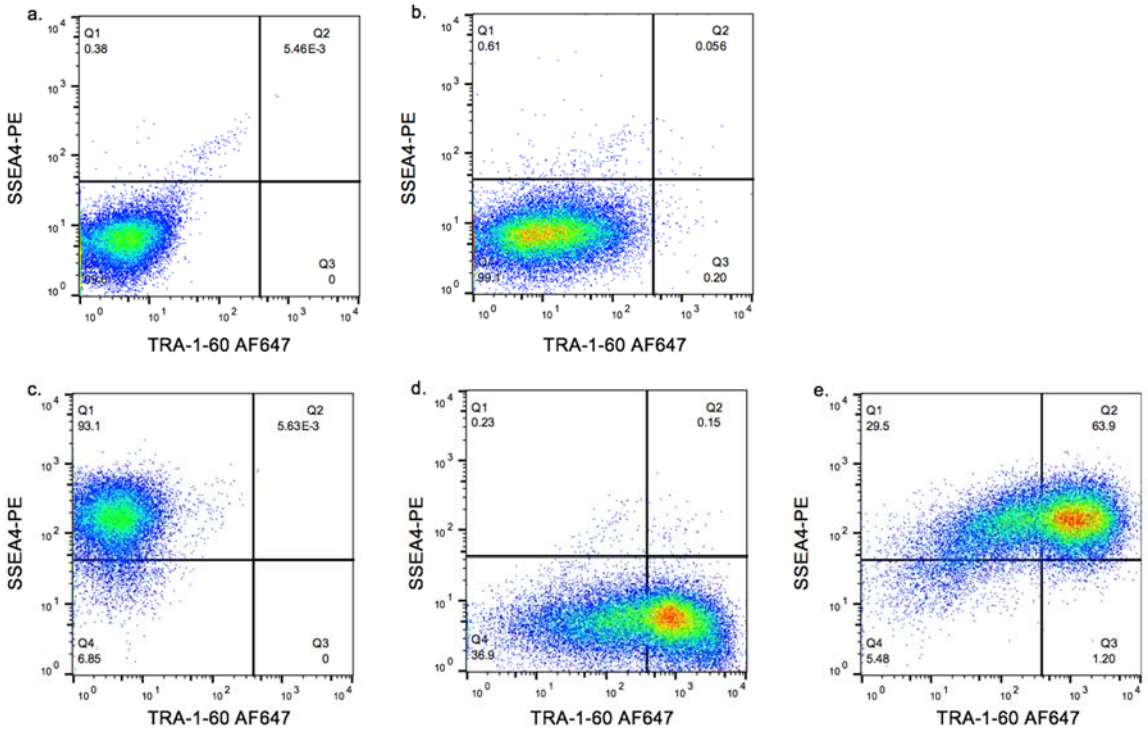

Figure C1. Flow cytometry analysis of episomally generated hiPSCs from one donor for the presence of TRA-1-60 and SSEA-4 markers at P5.

representing the unstained cells b) representing negative control (isotype control) of pluripotent markers c) representing cells stained only for SSEA4 pluripotent marker d) representing cells stained only for TRA-1-60 e) representing cells stained for both SSEA4 and TRA-1-60 pluripotent markers.